Master's thesis

NTNU
Norwegian University of Science and Technology
Faculty of Engineering
Department of Marine Technology

William Hyggen Viken

A method for evaluating the potential for retrofitting Wind Assisted Ship Propulsion from a ship owner perspective

Master's thesis in Marine Technology
Supervisor: Stein Ove Erikstad
June 2022

NTNU
Norwegian University of
Science and Technology

William Hyggen Viken

A method for evaluating the potential for retrofitting Wind Assisted Ship Propulsion from a ship owner perspective

Master's thesis in Marine Technology
Supervisor: Stein Ove Erikstad
June 2022

Norwegian University of Science and Technology
Faculty of Engineering
Department of Marine Technology

NTNU
Norwegian University of
Science and Technology

Master Thesis in Marine Systems Design

Stud. techn. William Hyggen Viken

“A method for evaluating the potential for retrofitting Wind Assisted Ship Propulsion from a ship owner perspective”

Spring 2022

Background

As the seaborne supply chains aim to become more decarbonized, Wind Assisted Ship Propulsion (WASP) is a potential technology for reducing fuel costs and emissions. As a result, there is a need for evaluating the potential of these technologies.

Overall aim and focus

The overall aim of the project is to develop a method that can be used by ship owners to evaluate cost and emission reduction by retrofitting WASP.

Scope and main activities

1. Provide a short overview of the current status and important development trends related to wind assisted ship propulsion.
2. Propose a step-by-step method for evaluating fuel savings.
3. Develop a case study based on AIS and metocean hindcast data.
4. Apply these data in the method and present potential savings based on the case study.
5. Discuss and conclude.

Modus operandi

Professor Stein Ove Erikstad will be the main supervisor from NTNU. The work shall follow the guidelines given by NTNU for the MSc Project work. The workload shall correspond to 30 credits.

Stein Ove Erikstad
Professor/Responsible Advisor

Preface

This master thesis is written within the course TMR 4930 - Marine Technology, Master's Thesis at the Department of Marine Technology at the Norwegian University of Science and Technology. The work corresponds to 30 credits and work has been conducted in the period between January and June 2022.

The thesis can be seen as an extension of the work conducted in the project thesis in the course TMR4560 - Marine Systems Design, Specialization Project. As a result, some of the material for the project thesis has been reused and revised to some degree. The sections of concern are mainly within the background study.

William Hyggen Viken williamviken@gmail.com

Trondheim, 09.06.2022

Acknowledgments

I want to thank my advisor, Professor Stein Ove Erikstad, for professional discussions and guidance concerning areas of interest in this master thesis.

Additionally, I would like to thank Benjamin Lagemann, Ph.D. candidate at NTNU, and Dražen Polić, Postdoctoral Fellow at NTNU, for valuable guidance and for providing relevant literature. They have also provided necessary software codes, essential for conducting the work that has been done.

At last, gratitude is extended to master student Finn Lorange, which is writing his thesis on the same subject, for encouraging and clarifying discussions throughout the semester.

Abstract

The shipping industry accounts for nearly 3% of the anthropogenic carbon dioxide emissions, and stakeholders within the shipping industry are currently under pressure to find solutions to reduce these emission. A concept presenting itself as a promising measure for reducing fuel consumption is Wind Assisted Ship Propulsion (WASP).

In the first part of this thesis, a literature study of 5 different WASP technologies was conducted. It was found that the Flettner rotor is the most favorable concept for three reasons. The system is relatively easy to operate as it only requires RPM adjustment. Secondly, it has a low effect on surrounding systems and the logistics due to its high lift coefficient. Finally, the technology has been tested for many years, resulting in well-documented effects and established suppliers.

Based on the background study, a method for evaluating the feasibility of installing Flettner rotors on a vessel as a preliminary effort was developed. The method uses vessel main particulars and the configuration of Flettner rotors as input to calculate the vessel's performance. With AIS data of previous routes and corresponding weather data, potential fuel savings are estimated for the route that has been sailed by the ship. This method calculates these savings based on the original operational profile and concepts of operations that are adapted to vessels fitted with WASP technology.

The method is applied to a case study of an 83 600 DWT LNG tanker fitted with five Flettner rotors with a height and diameter of 24m and 4m. Using the original operational profile of one year, the vessel can save 4.5%, corresponding to 127 kg/h MGO compared to the fuel consumption without WASP. Furthermore, the payback period is 7.2 years by using the average fuel price over the last two years. With current fuel prices, the payback period is reduced to 3 years.

Sammendrag

Skipsfart står for nesten 3% av de totale menneskeskapte utslippene av karbondioksid, og aktører innenfor den maritime næringen er under press for å finne løsninger for å redusere disse utslippene. Et lovende konsept for å imøtekomme dette problemet er Wind Assistert Skips propulsjon (WASP).

I første delen av oppgaven utføres det en litteraturstudie av fem ulike WASP løsninger. Det ble kommet frem til at Flettner rotoren er den foretrukne løsningen pga. tre grunner. Systemene er enkle å bruke, siden den kun behøver justering av omdreiningshastighet. Høy løft koeffisient bidrar til at den opptar mindre plass og dermed medfører få konsekvenser for omkringliggende systemer og logistikk. I tillegg så er det en godt utprøvd teknologi, med godt dokumentert effekt og etablerte leverandører.

Basert på bakgrunns studiet ble det utviklet en metode for å evaluere gjennomførbarheten av å etter montere Flettner rotorer på et skip i en tidlig fase av et prosjekt. Metoden bruker skipets hoveddimensjoner sammen med konfigurasjon av Flettner rotorer som input og regner ut ytelsen fra skipet. Ved hjelp av AIS (automatisk identifikasjonssystem) data fra tidligere ruter og tilhørende værdata, så kan ytelser som drivstoffbesparelse regnes ut for den faktiske ruten seilet av fartøyet. I tillegg så regner metoden ut potensiell drivstoffbesparelse dersom operasjonsprofilen tilpasses WASP fartøy.

Metoden ble brukt på en case-studie av et 83 600 DWT LNG tankskip montert med fem Flettner rotorer av størrelse 4x24m. Ved bruk av den opprinnelige operasjons profilen ble det estimert at skipet kan spare 4.5%, som tilsvarer 127 kg/h av det opprinnelige drivstoff forbruket av MGO. I tillegg ble tilbakebetalingsperioden for investeringen funnet til å være 7.2 år, med en drivstoffpris tilsvarende gjennomsnittet over de to siste årene. Med dagens drivstoff priser er tilbakebetalingsperioden redusert til 3 år.

Table of Contents

List of Figures

List of Tables

Nomenclature

List of Abbreviations

API	Application Programming Interface
AWA	Apparent Wind Angle
AWS	Apparent Wind Speed
CONOPS	Concept of Operations
SR	Spin Ratio
TWA	True Wind Angle
TWS	True Wind Speed
WAPS	Wind Assisted Propulsion System
WASP	Wind Assisted Ship Propulsion

List of Symbols

α	Hellman coefficient
θ_{AW}	Apparent wind angle
θ_{TW}	True wind angle
C_D	Drag coefficient
C_L	Lift coefficient
C_P	Power coefficient
$C_{L,drift}$	Lift coefficient due to drift
U_{AW}	Apparent wind speed
U_S	Incoming wind due to ship movement
U_{TW}	True wind speed

Chapter 1

Introduction

1.1 Background and motivation

As the consequences of climate change become more apparent, the world is transforming to become more climate-friendly. As a result, the shipping industry, which accounts for nearly 3% of the anthropogenic carbon dioxide emissions is currently under pressure to reduce emissions. Meanwhile, there is a rapid increase in the global demand for seaborne transport, whereas 90% of the world trade is currently carried by sea.

With the increase in shipping activity, the industry has increased its greenhouse gas (GHG) emissions. According to the fourth greenhouse gas study from 2020, the total GHG emissions from shipping have risen from 977 million tonnes in 2012 to 1076 million tonnes in 2018 (9.6% increase). The CO_2 emissions were 962 million tonnes and 1056 million tonnes respectively 2012 and 2018. These findings bring the share of shipping emissions in global anthropogenic emissions to 2.89% (IMO 2020). In 2018, IMO set a goal to halve the emissions from the world fleet compared to 2008 numbers (Joung et al. 2020). As a result, the interest in wind as propulsive power has been reignited.

In the wake of steam-powered ships' rise, the internal combustion engine and the availability of cheap fossil fuel, commercial sailing ships vanished. However, the interest in wind power as an important mode of powering commercial ships has spiked on several occasions since. In 1902, well after implementing steam and internal combustion engine, two commercial sailing vessels of both 8000 DWT were built. Even today, these still are the largest sailing vessels without an auxiliary engine ever built. The American built 7-masted schooner Thomas W. Lawson with a sail area of 3700 m^2 and the German-built Preussen with a total of 5600 m^2 sail area proved to be only marginally economically viable. In the end, they shared the same fatal fate as they were wrecked by accident in 1907 and 1910 (Wind ship development corporation 1981).

Until this century, these sailing vessels have been the symbol for the end of sails

on commercial vessels. However, several Wind Assisted Ship Propulsion (WASP) technologies have been proved to make the seaborne supply chain more resilient, decarbonized and cost-effective. The most important technologies are the Flettner rotor, wingsail, towing kite, suction wing and soft sail. These systems can reduce emissions from commercial shipping and act as a hedging instrument against fluctuating fuel prices for ship operators.

In addition to WASP technology, there are several additional measures for reducing emissions, such as alternative energy carriers, resistance reduction technologies and exhaust gas cleaning. For a ship owner that needs to decide on which technology to invest in, there is a need for a method consuming few resources as a preceding analysis.

1.2 Overall aim and focus

In this report, the main objective is to develop a method as a preliminary effort for evaluating the potential for retrofitting Wind Assisted Ship Propulsion. The method should take a ship owner perspective and investigate key performance indicators such as fuel consumption and sailing times for WASP vessels. Additionally, the proposed method should be easy to use for a ship owner. Hence, the procedure should only require available data as input and provide short computational times. Furthermore, the theory and methodology behind the method will be provided as well as the results when applying the methodology on a case study.

1.3 Outline of the thesis

This thesis is structured into 9 chapters. The introduction in Chapter 1 is followed by a description of different WASP concepts in Chapter 2 and operational concerns for WASP vessels in Chapter 3. Chapter 4 presents theory for WASP vessels, mainly sailing principles. A literature review of similar work is then presented in Chapter 5. These chapters forms the basis of the model and methodology in Chapter 6 which is performed on a case study where the results are displayed in Chapter 7. Second to last, Chapter 8 includes discussion of the findings obtained by the literature study and the methods used. Finally, Chapter 9 concludes the thesis and presents suggestions for further work.

Chapter 2

Wind Assisted Ship Propulsion concepts

The WASP technology consists of a wide range of concepts, such as Flettner-rotors, kites, suction wings, and aerofoils. These technologies have varying costs, benefits, restrictions and technological requirements. In this section, the drawbacks, advantages and technical properties of these concepts will be presented.

2.1 Flettner rotor

The rotor sail, or Flettner rotor, is a concept that dates back to the 1920s when German aviation engineer and inventor Anton Flettner started developing the rotor sail (Blueburd Marine Systems 2021). The Flettner rotor is a long cylinder that is rotated along its long axis, and as wind passes at a particular angle, force will be induced on the cylinder. This phenomenon is called the *Magnus effect*.

Investigating the Magnus effect, the force induced on the cylinder results from the pressure difference on each side of the cylinder. The pressure difference occurs when wind meets a spinning rotor sail. On the side where the cylinder is rotating against the wind, the airflow decelerates, and on the opposite side, the wind flow accelerates. Thus a force perpendicular to the wind flow direction is created, as displayed in Figure 2.1 (Norsepower 2021b). Variable rotor RPM allows for optimization of the Magnus effect over a range of wind conditions, which makes electric or hydraulic transmission favorable. Rotor RPM should be roughly proportional to the wind speed, meaning that the maximum rotor RPM limits the performance in strong wind conditions. The initial cost of installing the Flettner rotor rig increases with higher designed maximum RPM and thrust. The performance in high wind speeds is therefore a trade-off between initial costs and maximum load (Wind ship development corporation 1981).

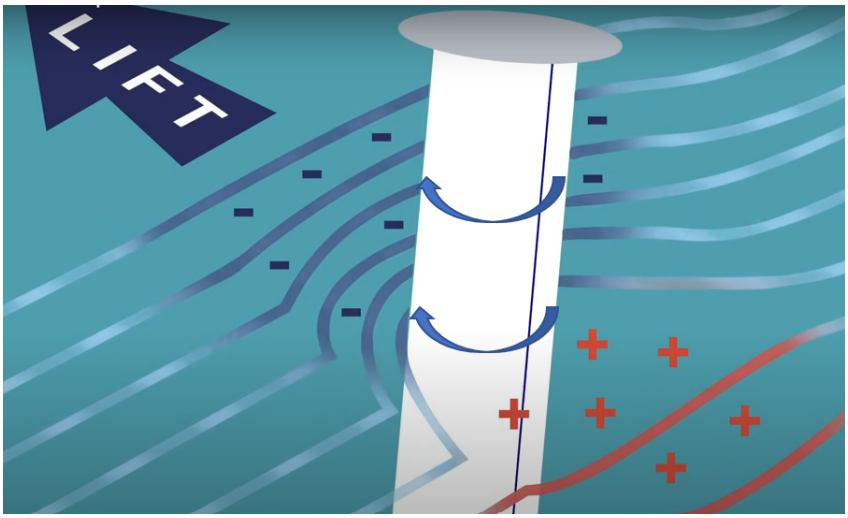

Figure 2.1: Magnus effect on rotor sail

Source: Norsepower 2021b

Over the past decade, the technology has been embraced by an increasing number of ship owners. In 2010, the 10500 DWT cargo ship Enercon E-ship 1 came into operation. The ship was fitted with four 25 m high, 4 m diameter rotor sails. Comparisons between operations with motor power only and with rotor sail operation show that up to 22.9% of the fuel consumption has been saved on the route between Emden and Portugal (Lu and J. Ringsberg 2020). According to Norsepower (2021a), the RO-RO vessel M/V Estraden has reduced fuel consumption and related emissions by 6.1% on the vessel's typical route after the rotor sail retrofit. The ship was fitted with two rotor sails with a height of 18 m and a diameter of 3 m in 2014 and 2015. In Table 2.1, vessels with rotor sails are listed.

Figure 2.2: SC Connector

Source: Seatrans 2021

Table 2.1: Recent Rotor sail adoptions

Ship name	Ship type	DWT	No. of rotors/ Height[m]/ Diameter[m]	Ship built year	Installation year
E-ship 1	Ro-Lo	10 020	4/27/4	2010	2010
Estraden	Ro-Ro	9700	2/18/3	1999	2014
Viking Grace	Passenger	6107	1/24/4	2013	2018
Adria Kvarner	General cargo	4250	1/18/3	1997	2018
Timberwolf	Tanker	109 647	2/30/5	2008	2018
Afros	Bulk carrier	64 000	4/16/2	2018	2018
Copenhagen	Ferry	5088	1/30/5	2012	2020
Annika Braren	general cargo	5100	1/18/3	2020	2020
SC connector	Ro-Ro	8843	2/35/5	1997	2020
Sea Zhoushan	Bulk carrier	324 268	5/24/4	2021	2021
MS Annika Braren	General cargo	5 035	1/18/3	2020	2021
MV Delphine	Ro-Ro	27 687	2/35/5	2018	exp. 2022

Source: Chou et al. 2021, Brouwer 2021, Ashmore 2022

2.2 Wingsail

Another promising concept for harvesting wind force as propulsion, are wingsails. Like a wing on an airplane, it uses aerofoils to generate lift and a strong propulsive force while decreasing the induced drag that slows down the ship. The sail can rotate 360 degrees for optimum angle of attack, meaning that the wingsail is versatile in different wind directions. Due to its pivot point being placed close to the leading edge, the wing will feather when allowed to rotate freely (Wind ship development corporation 1981). For the wings to be able to produce aerodynamic forces, the shape of the foil is adjustable. The wing could have a plain trailing edge, trailing edge plain flaps or trailing edge slotted flaps as shown in the air-foil cross-sections displayed in Figure 2.3.

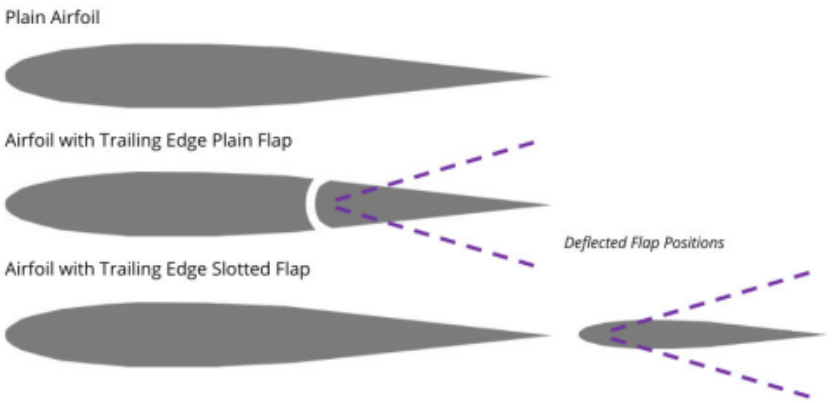

Figure 2.3: Rigid wingsail model configurations

Source: Reche-Vilanova et al. 2021

This technology already saw the light of day in the 1980s when the Japanese shipbuilder company Nippon Kokan started developing a rigid wingsail concept in the wake of increased fuel prices in the 1970s. The first vessel built was the coastal tanker Shin-Aitoku Maru (Figure 2.4), one out of 17 vessels fitted with the JAMDA (Japan Machinery Development Association) rig. Depending on wind conditions, the vessels reduced fuel consumption by around 10 to 30%. Despite achieving great results regarding fuel consumption, these sails could only be fitted on smaller types of vessels as the effects were low on larger and less slender hulls (Ariffin and Hannan 2020).

Figure 2.4: Shin-Aitoku Maru fitted with wingsails

Source: Ariffin and Hannan 2020

Today, the technology is far from the most common WASP technology, however, the concept has gained momentum in the past few years. The Hong Kong registered crude oil tanker from 1993 presented in Table 2.2, was fitted with two rigid wingsails in 2018.

Table 2.2: Recent wingsail adoptions

Ship name	Ship type	DWT	No. of sails/ Height[m]/ Width[m]	Ship built year	Installation year
New Vitality	Tanker	306 751	2/32/15	1993	2018
Canopee	General cargo	N/A	4/30/12	exp. 2022	exp. 2022

Source: Chou et al. 2021, Mackor and Pieffers 2021

2.3 Towing Kite

Utilizing lift from high altitude winds, kites can be used to provide thrust to a vessel. In contrast to other WASP concepts presented in this paper, this solution takes up negligible deck area and is relatively easy to install. Furthermore, there are no superstructures that can obstruct loading/offloading and sailing under bridges since the kite can easily be retracted. According to the manufacturer, the system is

housed in the forecastle area and installation takes only a few working days (SkySails 2021).

Today, commercial applications of towing kites are delivered by SkySails and Airbus-owned Airseas. The SkySails propulsion system consists of three main components: a towing kite, a launch/recovery system, and a control system for automated operation, which can be seen in Figure 2.5. According to Skysails, their kite can generate five to 25 times more thrust per square meter sail area compared to conventional sails. This is due to the automated control system commanding the towing kite to perform flight maneuvers. This increases the kite's airspeed to a multiple of the true wind speed. Additionally, the towing kites can operate between altitudes of 100 and 500 m where stronger and more stable winds prevail (SkySails 2021).

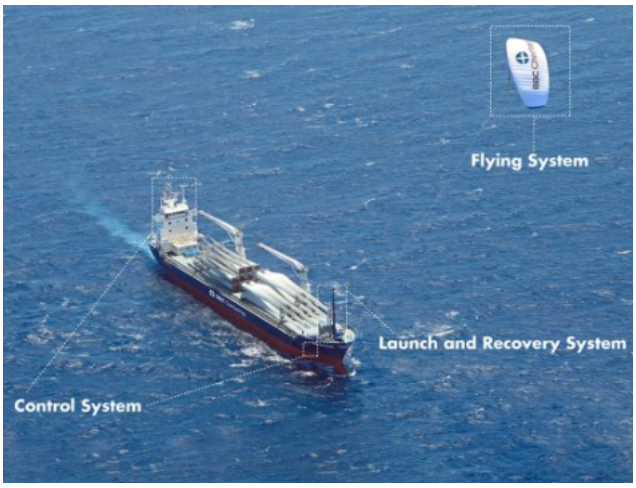

Figure 2.5: BBC Skysails fitted with towing kite

Source: SkySails 2021

As presented in Table 2.3, there are now four vessels sailing with this technology. These vessels were retrofitted or built with this concept between 2008 and 2012. The RO-RO vessel Ville de Bordeaux used for transporting airplane parts for Airbus on a 20+10 year contract is expected to be fitted with towing kite delivered by Airseas in 2022 (Wikipedia 2021a). According to Airseas, the vessel can reduce fuel consumption by 20% on average (Airseas 2021).

Table 2.3: Recent towing kite adoptions

Ship name	Ship type	DWT	Kite dimensions $[m^2]$	Ship built year	Installation year
Micheal A.	General Cargo	4884	160	1994	2008
BBC Skysails	General Cargo	9832	320	2008	2008
Theseus	General Cargo	3667	160	2009	2009
Aghia Marina	Bulk Carrier	28 522	320	1994	2012
Ville de Bordeaux	Ro-Ro	5200	500	2004	2022

Source: Chou et al. 2021

2.4 Suction Wing

Suction wings can be seen as a wing sail with boundary layer suction. By utilizing boundary layer suction with the use of vents and an internal fan, force on an airfoil is increased. To prevent or delay boundary layer separation, low velocity fluid is sucked from the bottom of the airfoil. Separation increases in line with increasing angle of attack, however, boundary layer suction retards the point of separation, thus reducing drag and increasing lift (Epifanov, V. M. 2011). This technology is delivered by Econowind and is fitted onto two vessels as shown in Table 2.4. Fuel savings and emission reductions are between 10 to 30%, depending on vessel type, number of suctions wings and wind conditions (Conoship 2021).

Table 2.4: Recent Suction wing adoptions

Ship name	Ship type	DWT	No. of wings/ Height[m]	Ship built year	Installation year
Ankie	General Cargo	3600	2/10	2007	2020
Frisian Sea	General Cargo	6477	2/NA	2013	2020

Source: Chou et al. 2021

Figure 2.6: General cargo vessel Ankie fitted with two suction wings

Source: Chambers, Sam 2020

2.5 Soft sails

Soft sails can be described as traditional sails with modern features. The most common version is the Dynarig which dates back to the 1960s when it was developed by German engineer Wilhelm Prölß. Compared to a traditional square-rigged clipper like the Preussen, it has twice the efficiency and can be controlled by a single person from the bridge. The Dynarig consists of freestanding rotating masts where the sails

can be furled into the masts. The Dynarig is yet to be seen in commercial shipping, however, it has been installed on two yachts, the Maltese Falcon and the black pearl (Wikipedia 2021b). In 2012, a conceptual multipurpose vessel named Ecoliner with Dynarig were designed (Figure 2.7), however the concept has not yet been realized, (Dykstra naval architects 2021).

Figure 2.7: Ecoliner concept with 4 Dynarigs

Source: Dykstra naval architects 2021

Chapter 3

Operational concerns

This chapter describes three different operational concerns for vessels fitted with WASP technology, that are important for a ship owner to consider. Firstly, Section 3.1 introduces important factors to investigate in a risk assessment, which is also mandatory to achieve class approval of the WAPS class from DNV. In Section 3.2, different operational modes that can be applied on a WASP vessel are presented. At last, economic concerns in terms of installation, maintenance and fuel costs are presented in Section 3.3.

3.1 Risk assessment of WASP

Introducing sails in commercial shipping poses new challenges in terms of risk. Passing under bridges and cranes together with severe weather and sea conditions will influence the operation and handling of the ship, safety and line of sight. To ensure an equivalent safety level compared to conventional ship types, it is necessary to perform a dedicated risk assessment for WASP systems and vessels fitted with these systems (Werner et al. 2020).

The DNVGL-ST-0511 standard issued by DNV in November 2019 is meant as an independent technical standard for designing and constructing a wind-assisted propulsion unit. It can also act as a procedural and technical basis for ships applying for the additional class notification WAPS. The standard considers a range of design principles, including risk assessment, where it is emphasized that the risk assessment should address all areas of design, equipment and operation. The aspects that should be included are severe weather (storm, ice), overspeed, vibrations, control system failure, component failure, fire, static electricity and human error (*Wind assisted propulsion systems* 2019).

3.2 Concept of operations

To investigate the performance and operational pattern of vessels fitted with wind assisted ship propulsion technology, it is essential to distinguish between different operational modes. Each operational mode has its drawbacks and advantages in terms of fuel consumption, sailing speed, transported tonnage and return on investment. These operational modes can be divided into constant speed sailing, constant engine load sailing, fixed sailing time and finally, an operational mode where engine power is only used at lower speeds.

Firstly, the constant speed sailing is an operational mode where the vessel's speed is kept constant, and the power from the engine is decreased accordingly with more favorable wind conditions. This is typical for ships sailing within fixed schedules such as the RO-RO vessels M/V Estraden and SC Connector. This operation will also be beneficial for other vessels as they often have a particular design speed.

Moving on to constant engine load sailing, the operational mode assumes constant engine load where fluctuating wind conditions result in variable sailing speeds. The reason for using this particular mode can be to keep the engines operating at optimal load to ensure the lowest possible fuel consumption per produced unit of power (g/kWh). In addition, this mode can typically be used when a vessel is late for its destination. It will then be favorable to increase the sailing speed by raising the engine load in addition to gaining speed from the WASP technology. This operational mode is advantageous when the vessel is late for scheduled offloading/loading at port to avoid time penalties, loss of reputation or when the loading is served as a first in, first out (FI-FO) que.

The constant sailing time operation means that a fixed sailing time is set for the voyage, however the speed during sailing can be adjusted. In today's shipping industry, there are often strict schedules for transporting goods, and there are often penalties associated with late deliveries of cargo. In addition, the more expensive the cargo is, the more rapidly the cargo owner would want the shipment to be delivered to reduce tying up capital at sea. Although there are some challenges related to this type of operation, there are great possibilities for saving fuel. By planning the sailing speed for the whole leg by using weather forecasts, one can ensure that the vessel is sailing faster when wind conditions are favorable and subsequently reduce the sailing speed in calm weather. Using this operation, one can reduce the fuel consumption and still comply with the time windows.

The final operational mode is a bit more conceptual and relies on changing the marine logistics chain as we know it today. Here, engine power is only used when wind conditions are poor, and sailing speed is reduced to a set limit. The operational mode is suitable for WASP concepts that can generate a lot of lift so that wind can be the only source of propulsion for the majority of the sailing distance. In theory, this can be accomplished by several of the WASP technologies, regardless it will mean tying up a considerable amount of deck space. For now, soft sails have been the preferred sail type for this operational mode (Perez et al. 2021).

3.3 Economic impact

Shipping is an energy-intensive industry where fuel costs accounts for a large amount of its operating costs. Hence, reducing fuel consumption is of great importance from a shipowner/operator perspective. From an economic point of view, installing sails on a commercial vessel can have great potential to save fuel costs. However, the installation of a WASP device calls for a large investment cost and increased operational risk that must be justified by being repaid throughout the rest of the vessel's lifetime.

In Kolk et al. (2019) and Seddiek and Ammar (2021), buying costs and maintenance costs are provided by NorsPower for a 4x24m Flettner rotor. The costs in Table 3.1 are from 2019, however, they provide a reasonable estimate of relevant expenses.

Table 3.1: Flettner rotor costs

Specification	Value	Unit
Height	24	[m]
Diameter	4	[m]
Weight	43	[ton]
Buying cost	750 000	[USD]
Maintenance cost	10 000	[USD/year]
Lifetime	25 +	[years]

Source: Kolk et al. 2019, Seddiek and Ammar 2021

For the investment to be repaid during the remaining lifetime of the vessel, is highly dependent on the fuel price. In Figure 3.1, the MGO bunker price for Rotterdam (red) and a global 20 ports average (grey) is presented for a three-year period between April 2019 and April 2022. The average trading price of the global 20 ports average was 606$ per metric tonne, and the lowest and highest prices were 270$ and 1247$ per metric tonne.

Figure 3.1: Bunker price of MGO at Rotterdam and 20 ports average

Source: Ship and bunker 2022

These volatile bunker prices can be traced back to the pandemic and a recent geopolitical issue in eastern Europe. These situations might be short-lived from a vessel lifetime perspective of around 25 years, however future fuel prices are uncertain. Therefore, installation of WASP devices can act as a hedging instrument against fluctuating fuel prices.

Chapter 4

Theory

The following chapter presents sailing theory for WASP vessels. Since the method in Chapter 6 is used to calculate the effects of Flettner rotors, this chapter has a bias toward Flettner rotor theory.

4.1 Force generated by WASP systems

The forces generated by WASP systems can be investigated further by looking at the net force acting on the sails, which consists of drag (D) and lift (L). The lift is acting perpendicular to the local apparent wind direction, and the drag force is acting in line with the apparent wind direction (Kramer 2014). The relation between the apparent wind and true wind is shown in Figure 4.1.

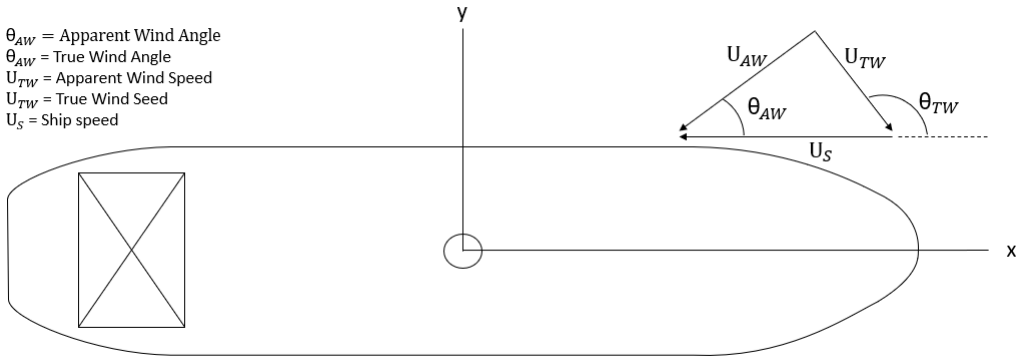

Figure 4.1: Relation between ship velocity, true wind and apparent wind

The true wind, also known as ground wind, is the wind experienced from a stationary perspective. Apparent wind is the wind that is experienced from a moving vessel perspective. The mathematical formulation for calculating the apparent wind speed U_{AW} and the apparent wind angle, θ_{AW} is presented in respectively Equation 4.1 and Equation 4.2, where θ_{TW} is the true wind angle.

$$U_{AW} = \sqrt{U_{TW}^2 + U_S^2 + 2 \cdot U_{TW} \cdot U_S \cdot cos(\theta_{TW})} \tag{4.1}$$

$$\theta_{AW} = arccos\left(\frac{U_W \cdot cos(\theta_{TW}) + U_S}{U_{AW}}\right) \tag{4.2}$$

To investigate the thrust and side force, the coordinate system is converted so that the x-axis is pointing in the direction of travel for the ship, as displayed in Figure 4.2.

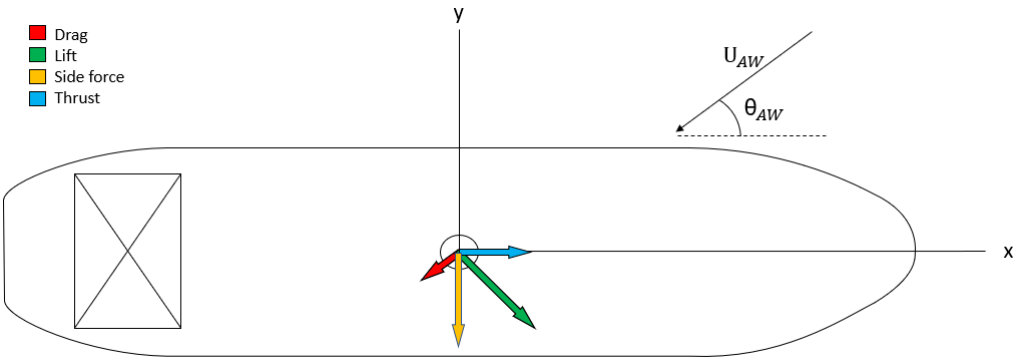

Figure 4.2: Schematic of forces and apparent wind

The lift coefficient C_L and drag coefficient C_D can then be converted into thrust coefficient C_T and heel coefficient C_H, by using the local apparent wind direction α, as shown in Equation 4.3 and Equation 4.4.

$$C_T = C_L \cdot sin(\theta_{AW}) - C_D \cdot cos(\theta_{AW}) \tag{4.3}$$

$$C_H = C_L \cdot cos(\theta_{AW}) + C_D \cdot sin(\theta_{AW}) \tag{4.4}$$

The thrust force (T) and force from heel (H) can then be calculated based on the sail area (S), apparent wind speed (U_{AW}), air density (ρ), heel coefficient (C_H) and thrust coefficient (C_T) as shown in Equation 4.5 and Equation 4.6. The projected sail area (S) for the Flettner rotor is calculated as $S = H \cdot D$ (Lu and J. Ringsberg 2020).

$$T = C_T \frac{1}{2} \rho U_{AW}^2 S \tag{4.5}$$

$$H = C_H \frac{1}{2} \rho U_{AW}^2 S \tag{4.6}$$

4.2 Lift coefficient on a spinning cylinder

To calculate the lift coefficient (C_L) of the Flettner rotor, a theoretical lift coefficient can be found using the Kutta-Joukowski theorem of lift by substituting the expression of lift from the dimensionless lift coefficient into the equation, where Γ is the circulation induced by the spinning cylinder.

$$F_L = \rho \Gamma U_{AW} H \tag{4.7}$$

By assuming $\Gamma = 2\pi RU$ where $U = \omega R$, the lift coefficient can be found in Equation 4.8. U is the velocity of the cylinder surface and ω is the angular velocity (Reche-Vilanova et al. 2021).

$$C_L = 2\pi U/V, \quad where \quad U/V = \frac{\omega R}{U_{AW}} \tag{4.8}$$

In Prandtl and Betz (1932), the drag and lift coefficients are measured as a function of velocity ratio for two cylinders with an aspect ratio (H/D) of 1.68 and 12. The measurements were also done with different end plate diameter ratios (end plate diameter/rotor diameter) of 1, 1.5, 2 and 3. The results are shown in figure Figure 4.3.

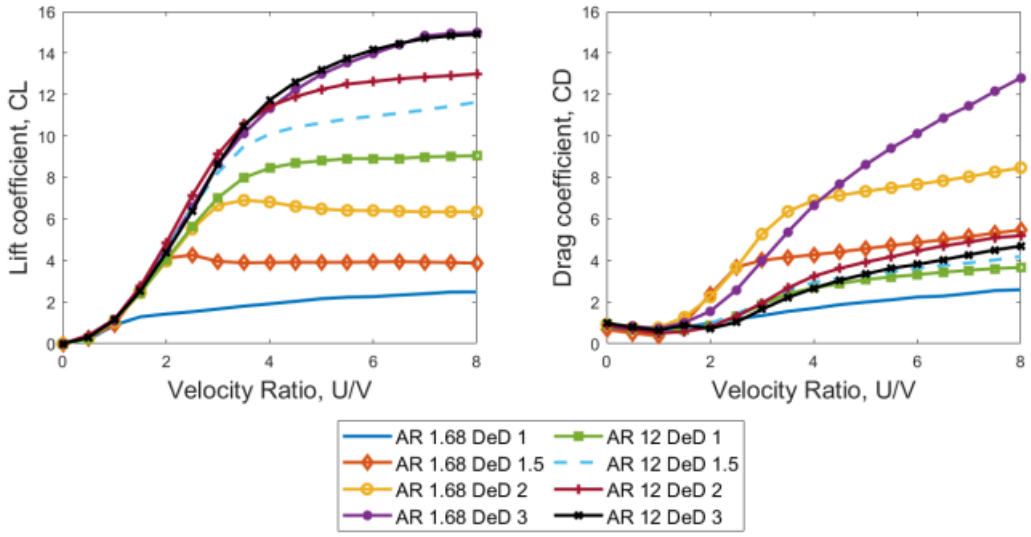

Figure 4.3: Lift and drag coefficients for cylinders

Source: Reche-Vilanova et al. 2021

In figure Figure 4.3, the results regarding the cylinder with an aspect ratio of 12 are most relevant for a Flettner rotor. At the highest velocity ratio of 8, a maximum lift coefficient of 11.6 is reached for the cylinder with a 1.5 end plate diameter ratio. The corresponding drag coefficient is found to be 4.0.

4.3 Wind speed profile

Allthough the Rotor sail can generate significant thrust per square meter due to its high lift coefficient, the thrust generated is not equally distributed along with the height of the cylinder. As a consequence of the friction between the earth's surface and flowing air, a boundary layer is created. The boundary layer shape and thickness are affected by the roughness of the surface and air turbulence. In addition to altering wind speed along with the height of the sail, the wind angle is also dependent on the height above the deck (Tillig and J. W. Ringsberg 2020).

The resulting wind speed gradient can be formulated as (Kaltschmitt et al. 2007):

$$TWS(h) = TWS_{10}(\frac{h}{h_{10}})^{\alpha} \tag{4.9}$$

TWS_h is the true wind speed at height h and TWS_h is the true wind speed at the corresponding h_{10}, which is the height of 10 m. α is the Hellman coefficient which is a relation between the turbulence of the wind and the surface of the earth/sea.

In Tillig and J. W. Ringsberg (2020), the wind profile for a 30 m Flettner rotor is calculated. The height of the deck is set to 14 m, TWS_{10} is 7.3 m/s, TWA is 60° and vessel speed is ten knots. The results displayed in Figure 4.4 show that the speed is 60% higher at the top compared to the bottom, while the apparent wind angle is 3° larger.

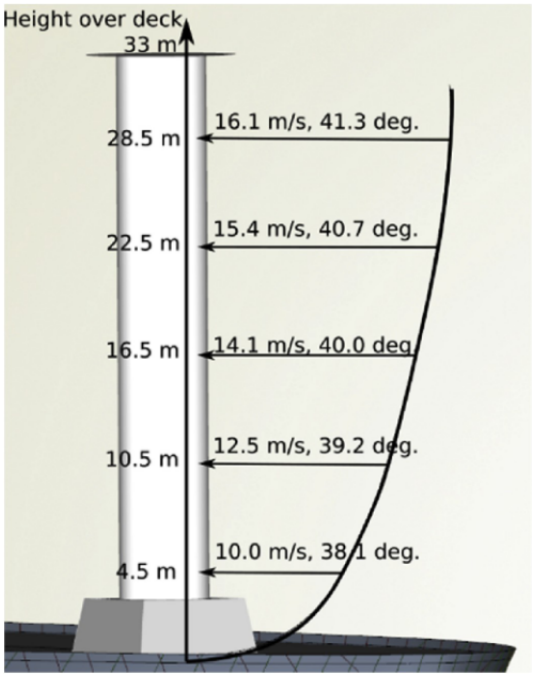

Figure 4.4: Wind speed profile and apparent wind angle

Source: Tillig and J. W. Ringsberg 2020

4.4 Fuel consumption

To estimate the costd and emissions reduction, it is essential to accurately estimate the fuel consumption. The formula presented in Equation 4.10 is used to calculate the fuel consumption per voyage.

$$F = \Sigma_{i=0}^{n} \left(\frac{D_i}{v_i} \cdot (K_f \cdot P_i) \cdot \left(1 + \left(0.7 - \frac{P_i}{P_{tot}} \right)^2 \right) + (K_{aux} \cdot P_{aux}) \right) \tag{4.10}$$

To account for varying sea conditions, the voyage is divided into n sailing sections with a distance D_i, sailing speed v_i and required power P_i for sailing section i. K_f represents the fuel consumption per produced kWh at the engine's most optimal load and P_{tot} is the total installed power. The part of the code represented by $\left(1 + \left(0.7 - \frac{P_i}{P_{tot}} \right)^2 \right)$ estimates high fuel consumption per produced kWh at low power, a close to linear curve between 55% and 85% of max power, and a gradual increase up to maximum engine load. This approximation provides a sufficient replication of the performance of a typical diesel engine. At last, $K_{aux} \cdot P_{aux}$ represents the fuel consumption for auxiliary loads such as the hotel load (Lindstad et al. 2022).

4.5 Power consumption of Flettner rotor

The Flettner rotor is powered by an electrical motor to spin and generate lift. The additional power consumed by the Flettner rotor can be expressed by a power coefficient C_P, as shown in Equation 4.11 (Tillig and J. W. Ringsberg 2020).

$$C_P = \frac{P_{rotor}}{0.5 \cdot \rho \cdot A \cdot U_{AW}^3} \tag{4.11}$$

Chapter 5

Comparable WASP studies

Before conducting own research and analysis it is important to get an overview of work and literature within the field of wind assisted ship propulsion. Doing so will give valuable insight into possible methods for this thesis and indicate results to be expected, for validation purposes.

Already in the 1970s, researchers saw the potential for reducing fuel consumption using wind. Motivated by world developments in energy supply and environmental concerns, the feasibility of sailing ships for the American merchant marine is studied in Woodward et al. (1975). Three ships of 15 000, 30 000 and 45 000 DWT, both wind and engine powered, are compared with similar traditional vessels based on economic performances on a range of deep-sea shipping routes. The study's objective is not to find the best WASP technology, and as a result, the scope of the study only approved for one sail technology to be analyzed. As a sailing ship, the operational mode is only wind power with speeds above 6 knots. Auxiliary power is only used when sailing slower than 6 knots and maneuvering in harbors. Inspired by the sailing vessel Preussen, modern soft sails similar to today's Dynarig are chosen for the study. The total sail area for the vessels was respectively 8180, 12920 and 16638 m^3. Auxillary engine power was set to 600 hp, 1000 hp and 1200 hp. At the time, no similar vessel had been built and the authors referred to the concepts as preliminary designs and the "first loop in the design spiral". The concept, with corresponding sail configuration is displayed in Figure 5.1.

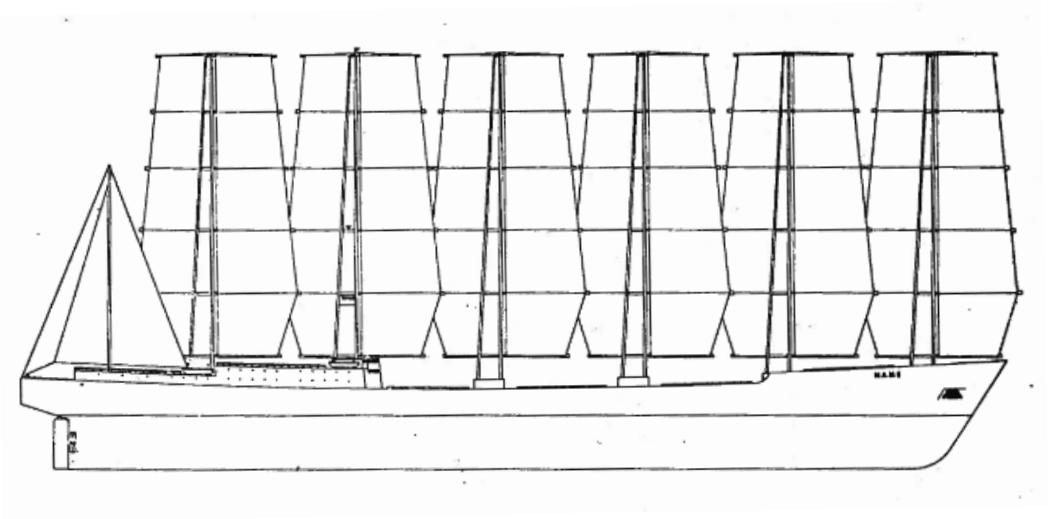

Figure 5.1: 45 000 dwt bulk cargo ship with Dynarig

Source: Woodward et al. 1975

The authors calculated pre-set sailing voyage tracks based on average wind speeds and directions. By using Dynarig force coefficients and Mariner hull leeway force coefficients together with Resistance curves from Series 60 motor vessel hull forms, speed polar curves for each vessel were generated. Average crossing speeds with variances could then be calculated for each voyage and season using the Monte Carlo method to randomly pick local wind speeds and wind directions based on statistical weather data (Perez et al. 2021). Voyage costs could then be calculated together with building costs and operational costs. Building costs for the sailing vessel are found to be 10% higher than for a conventional steamer.

The required freight rate (dollars per ton) is then computed for every vessel and route. The study finds that with one exception, all entries favored the conventional engine-powered ship. The exception occurs on the most extended voyage with the smallest vessel. As a result, the conclusion is that commercial sailing ships are not competitively superior to engine-powered ships. However, it is discussed that a potential future rise in energy costs might tip the results in the sailing vessel's favor.

Forty-six years after, this is precisely what has happened. In Perez et al. (2021), the report from 1975 has been updated with today's costs to find that sailing merchant vessels are more profitable compared to regular steamers. By estimating updated building costs, fuel prices, crew costs, insurance rates, maintenance and repair costs, overhead costs, stores and lubes costs, port costs and financial charges for the exact vessel sizes, the required freight rate is found to be between 21% and 40% lower than the equivalent motor vessel, depending on the ship and route. In Figure 5.2, required freight rates for a 45 000 DWT vessel are shown for four different routes. Compared to a conventional engine-powered vessel of the same size, the building costs are 20% higher, and emissions are reduced by approximately 90%. Calculations show that the concept is resistant to fluctuating prices. For the motor vessel to outperform the sailing vessel, fuel prices will have to dip below $40-50/barrel, or the building costs will have to rise above 50% higher than the construction costs of the motor vessel.

HFO costs in this study were set to \$63/barrel, while the recent ten year average is \$72/barrel.

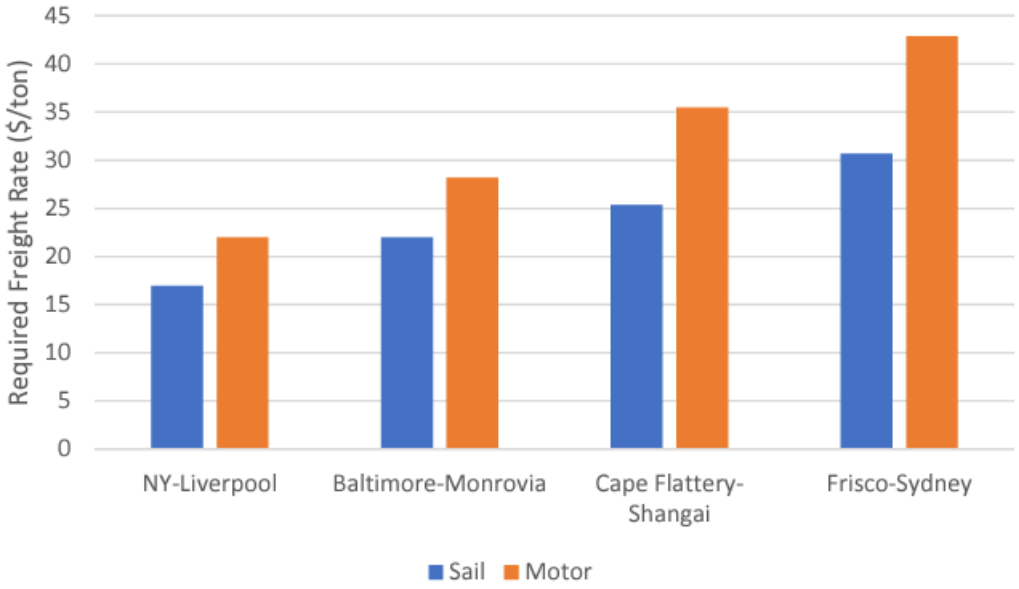

Figure 5.2: Required freight rate for sail and wind-powered 45 000 dwt bulk cargo ship for four different routes

Source: Perez et al. 2021

The average velocities were found to be respectively 9.2, 9.8 and 10.5 knots, however the engine is used for approximately 50% of the distance traveled in the summer due to unfavorable wind conditions. Thus, the increase in sailing times during the summer months is far from negligible. This will require a more flexible delivery schedule (Perez et al. 2021).

Moving on to other WASP technologies, the fuel saving performance of three different WASP technologies is investigated in Lu and J. Ringsberg (2020). An Aframax oil tanker is chosen for a case study comparing Flettner rotors, Dynarig softsails and wingsails. At first, the ship performance simulation model calculates calm water resistance, shallow water resistance, propeller design with corresponding performance curves, propulsive factors and engine data. The inputs in the model are basic ship information inputs, such as ship type, number of blades, propeller RPM, engine speed, design speed, etc. The voyage can then be simulated using historical weather data at waypoints along the route and operational modes such as fixed target speed, fixed journey time and fixed engine load. At last, the contributions from the sail technologies are calculated based on the formulas in Section 4.1 and corresponding lift and drag coefficients.

The fuel saving performance of the WASP technologies could then be estimated. The sail area of the wingsail and Dynarig were set to 1000 m^2, whereas the two Flettner rotors were designed to be 18 m in height and 3 m in diameter, corresponding to a total surface area of 509 m^2 and projected area of 108 m^2. The maximum rotational speed was set to 600 RPM. Using a fixed time operational mode, the savings for the

voyage between Cape Lopez (Gabon) and Point Tupper (Canada) were found to be 5.6% for the Dynarig, 8.8% for the wingsail, and 8.9% for the Flettner rotor. For the voyage between Angro dos Reis (Brazil) and Rotterdam (The Netherlands), the fuel savings were found to be respectively 4.2%, 6.1% and 6.5%.

The study also conducts a parametric analysis of the Flettner rotor to investigate the sensitivity in the positioning of the rotor, rotational speed, vessel speed, vessel size and rotor dimensions. It is found that the rotor has better performance when placed on the fore part of the ship and with smaller vessels (Aframax oil tanker vs. Handysize bulk carrier). As expected, reducing service speed will have a positive effect on fuel consumption, whereas increasing maximum rotor speed contributes to a slight decrease in fuel consumption. It is also found that higher rotor speed and larger rotors do not always reduce fuel consumption. It is therefore concluded that it is necessary to select and operate the Flettner rotor according to ship type, speed, routes and weather conditions.

In Reche-Vilanova et al. (2021), a six degrees of freedom (DoF) Performance Prediction Program (PPP) is developed to predict the performance of three different WASP systems. As in Lu and J. Ringsberg (2020), these are the Flettner rotor, wingsail and Dynarig. The model uses only ship main particulars, general dimensions and weather data as input, so that the approach can be used during early-stage feasibility studies. Gravity forces, hydrostatic forces, aerodynamic forces and hydrodynamic forces are used to calculate the RPM, leeway angle, sinkage, heel angle, pitch angle and rudder angle using force and moment equilibrium. An outer loop of the algorithm then calculates trim parameters such as Angle of Attack (AoA), flap deflection angle or rotor sail RPM to optimize the WASP performance. The thrust is then computed using similar calculations as presented in Section 4.1 and engine RPM is reduced correspondingly. The outputs, including free variables, trim variables, polar plots and power savings are presented. For the free variables, the resulting sinkage and trim angle are found to be very small and the difference compared to using a 4 DOF system as proposed in Lu and J. Ringsberg (2020) would have been negligible. A general outline of the model is presented in Figure 5.3.

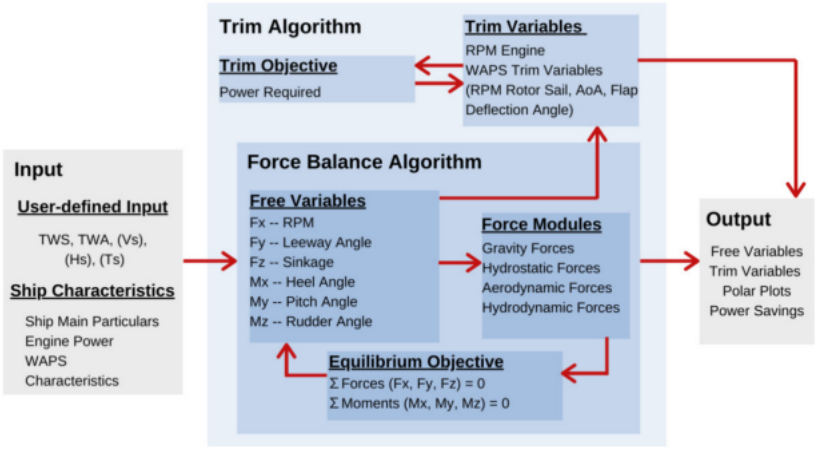

Figure 5.3: Schematic general outline of the Performance Prediction Program

Source: Reche-Vilanova et al. 2021

The predicted power savings for a vessel similar to "Maersk Pelican" (presented in Table 2.1) with two rotor sails, two wingsails (plain airfoil, plain flap, slotted flap) and Dynarig is compared at a wind speed of 10m/s and vessel speed of 8 knots in Figure 5.4. The same plots are constructed for different vessel speeds and wind speeds. It is found that varying sailing speed does change the magnitude of the savings, however it does not result in relative performance of the WASP systems. Nevertheless, higher absolute savings but a lower percentage of savings is achieved when increasing service speed. The Flettner rotor show higher fuel savings compared to other WASP systems, however the rotor is restricted by the maximum RPM and therefore shows lower fuel savings at higher wind speed.

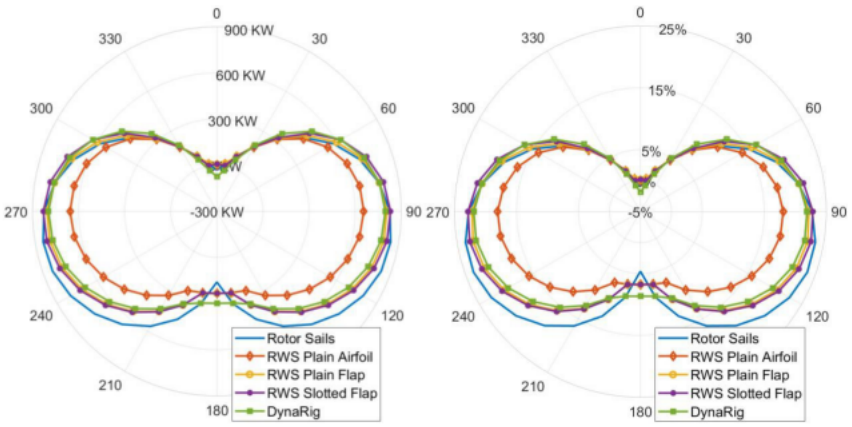

Figure 5.4: Power savings polar diagrams for different WASP technologies. Left: absolute power savings in kW. Right: power savings in percentage of total engine power required.

Source: Reche-Vilanova et al. 2021

Chapter 6

Method

This chapter presents the methods used in this thesis. At first, the vessel used in the case study is presented in Section 6.1, followed by how the AIS data is used to map the operational pattern of the vessel in Section 6.2. Then a method for collecting weather data and estimating the effects of a vessel fitted with Flettner rotors is presented. At last, the process of combining the weather data and effects from the rotor sail, and deriving the results is described in the final sections. A simple schematic of the method is shown in Figure 6.1.

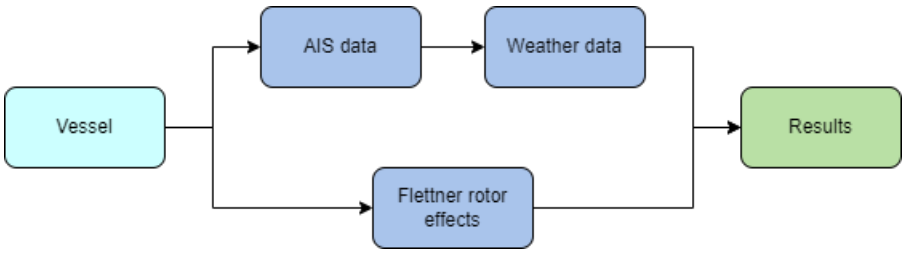

Figure 6.1: Outline of the method

6.1 The vessel

The vessel that will be used for this case study is an 83 636 DWT Moss type (spherical LNG tanks) LNG tanker. Being built in 2019, it is a modern vessel where its dimensions is designed to enable passage through the newly expanded Panama Canal, which opened in 2016. The ship will primarily be used to transport LNG produced via the American Cameron LNG project, however hull dimensions were preserved to enable docking at major LNG terminals around the world. Furthermore, the tank capacity of the LNG tanker is 156 000 m^3 (Kawasaki 2019).

The vessel has a 4-stroke, diesel electric propulsion system with a total of 4 dual fuel engines from Wärtsila (2x8L50DF and 2x9L50DF) producing a total of 31 800 kW at 514 rpm. The engines are connected to two electric motors of 11 980 kW each, which powers two fixed pitch propellers. Top speed with this installation is 21.6

knots and service speed is 14 knots with a rated fuel consumption of 50.0 tonnes per day (Sea-web 2022). More of the vessel particulars can be found in Table 6.1. The block coefficient and propeller diameter is assumed based on the vessel particulars, since they could not be obtained.

Table 6.1: Main Particulars

Length over all	L_{OA}	[m]	299.9
Length between perpendiculars	L_{PP}	[m]	286
Beam	B	[m]	48.9
Draught	T	[m]	11.829
Depth/top deck height	D	[m]	22.2
Deadweight	DWT	[tons]	83 636
Gross tonnage	GT	[tons]	128 917
Bulbous bow			yes
Block coefficient	C_b	[-]	0.75
Maximum ship speed	V_{max}	[knots]	21.6
Total installed propulsion power	$P_{ME}total$	[kW]	31 800
Propeller diameter	D_{prop}	[m]	8
Number of propeller shafts	N_{shaft}	[-]	2

Source: Sea-web 2022

In addition to the main particulars, the data for powering and fuel consumption are presented in Figure 6.2a and Figure 6.2b. This is used for calculating the fuel consumption at different sailing speeds. Optimal engine load is at 80% with a specific fuel consumption of 170 g/kWh.

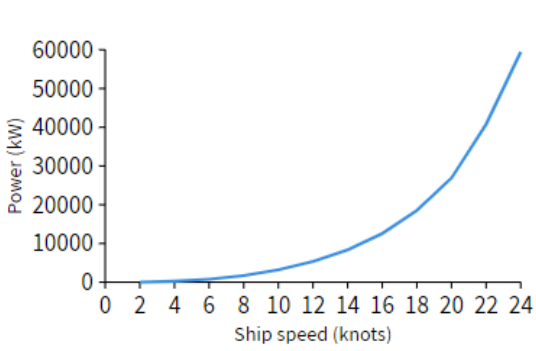

(a) Ship speed vs. power

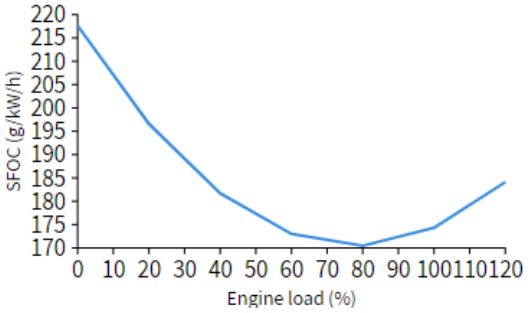

(b) Specific fuel consumption vs. engine load

Source: Lloyd's Register Advisory Services BV 2020

Originally, the vessel is not fitted with a WASP device. For this case study, five Flettner rotors with the specifics shown Table 6.2 are applied. The specifics are calculated based on the rotor height, diameter and linear interpolation of specifics from known Flettner rotor dimensions produced by the three manufacturers, NorsPower, Eco Flettner and Anemoi. These dimensions are chosen as result of having available costs for this Flettner rotor, which were presented in Table 3.1. By using five rotors,

the total sail area is 1508 m^2, which corresponds to the sail area of vessels of similar size listed in Table 2.1.

Table 6.2: Flettner rotor specifics

Height	24	[m]
Diameter	4	[m]
Sail Area	301.6	[m^2]
Max rotor speed	225	[rpm]
Base height	2.5	[m]
Weight	43.1	[tonnes]
Installed power	84	[kW]
Max thrust	177.6	[kN]
Number of rotors	5	[-]

It is worth mentioning that the reason for using this particular vessel for the case are not the characteristics of the ship itself, but its operational profile. With the characteristic deck space of a Moss type LNG tanker, placement of the rotors and interaction effects from bound vortex could pose challenges for a Flettner rotor retrofit, however the vessel sails on commonly used shipping routes that will provide performance data for a wide range of areas.

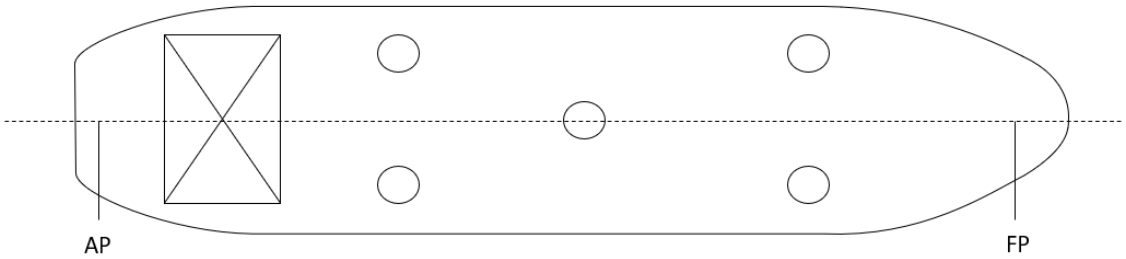

Figure 6.3: Flettner rotor configuration

6.2 Analysing the AIS data

Vessel location data from GPS or Automatic Identification System (AIS) can be used for real time tracking of the vessels, which later can be analyzed together with environmental conditions such as weather fronts, tides and current streams. The information from the AIS data that will be used in this thesis is mainly longitude, latitude, date time, speed over ground and heading. These data points are used for evaluating the operational profile, including speed profile and routes. They also form the basis of the way points used when analyzing the same vessel retrofitted with Flettner rotors.

Before the vessel performance is analyzed, the data is cleaned by removing duplicates and registrations of speed over ground that is higher than 25 knots. The longitude

and latitudes is then plotted on a map to ensure that there are no unexpected deviations of the route due to errors in the dataset. In addition to the need of cleaning the dataset, there are several potential drawbacks of using this approach. Firstly, loading conditions are not included in this dataset, which could have provided a more accurate estimation of the resistance and corresponding fuel consumption. Additionally, the vessel could have used weather routing, resulting in the waypoints to potentially be less optimal for a vessel fitted with WASP technology.

6.3 Collecting weather data

To be able to estimate the effects of WASP, it is necessary to acquire weather data for the time the vessel was at each specific location. Since the vessel sails on routes all over the world it was essential to find a database for weather data with global coverage. In this case, the European Union's Earth Observation Programme, Copernicus, is used. The Copernicus Climate Change Service (C3S), which is operated by European Centre for Medium-Range Weather Forecasts (ECMWF) were found to be a favorable solution as it provides an extensive database of past, present and future climate data such as wind speed, wind direction, wave period, wave direction and wave height. The data combines hindcast (observations) and analysis synthesized by their models (Selen, T. 2020).

The service also supports programmatic access to its Climate Data Store through its application programming interface (API). By using the programmatic access, the Python code in Lagemann (2022) and Section A was used to iterate through the AIS data and retrieve weather data based on longitude, latitude and time. Initially, the code accessed both wave and wind data from The Climate Data Store, however, since the Matlab code presented in Section 6.4, calculating the effects of Flettner rotors did not include wave data, it was excluded from the Python code. Due to the database's slow remote server database API, the run time for the Python code where then halved from taking 20 seconds to 10 seconds per iteration. With 206 000 data points, the run time would be just on the short side of 24 days. To further reduce the run time to a more acceptable level, the code was modified to fetch wind data for points with a minimum time difference of 6 hours.

The Climate Data Store provides access to several weather databases, however, it was decided to use the *Global Ocean Wind L4 Reprocessed 6 hourly Observations* database as it provides a broad coverage, both geographically and historically. More specifically, the database has a temporal range from 1992-01-01 to 2020-12-31. Although it does not provide data for the latest 1.5 years, the database is updated regularly (E.U. Copernicus Marine Service Information 2021).

6.4 Estimating the effects of Flettner rotors

After collecting the weather conditions experienced by the ship, the effects of the Flettner rotors can now be calculated using the model developed in Lindstad et al.

(2022). Compared to a regular non WASP vessel where a third order polynomial can describe the power consumption as a function of ship speed, the power consumption on a WASP vessel is more intricate. Although this model makes several simplifications, it is still necessary to account for many variables to achieve an accurate estimate. One of the simplifications is to ignore heave, pitch and heal, leaving a 3 DOF system to be analyzed. The fundamental objective of the code is therefore to estimate the drift angle due to yaw, resulting in a different surge speed and ship speed which, increases the resistance of the vessel.

At first, the Matlab code iterates through every increment of wind speed and ship speed and calculates the hydrodynamic derivatives, Y, based on the hull particulars (LWL, beam, draught, block coefficient and ship speed). These derivatives are calculated based on tuned nonlinear lift expressions, as done in Tillig and J. W. Ringsberg (2020). The lift coefficient for the lift and drag generated by the drift angle, β, can then be derived by an empirical method for maneuvering shown in Equation 6.1, which is based on Kijima et al. (1990). These coefficients increase to the power of two as a function of ship speed. As a result, the vessel's ability to produce lift and withstand side forces increase with higher ship speed. The normalized yaw angular speed, r, is zero for a straight course. Hence, the only derivatives that are used are Y_β and $Y_{\beta\beta}$.

$$C_{L,drift} = Y_\beta \beta + Y_{\beta\beta}\beta|\beta| + Y_{rr} r|r| + (Y_{\beta\beta r}\beta + Y_{\beta rr} r)\beta_r \tag{6.1}$$

The code then iterates over all the wind angles, which are set to be between 0 and 180 degrees with an iteration step of 2 degrees. The first restriction is that the drift angle must be smaller than 10°. Secondly, it checks if the wind is below 35 m/s at the tip of the Flettner rotor. The code then estimates the mean value of the wind speed on the rotor, and based on the mean value, the rpm of the rotor is determined. Now the code iterates through different rotor rpm's with a step of 5 rpm. For each iteration, the lift coefficient, drag coefficient and power coefficients are calculated based on the aspect ratio, diameter ratio, spin ratio and lift-drag coefficient of the Flettner rotor.

Furthermore, the preferred method for calculating lift and drag coefficients is set to the one used in Tillig and J. W. Ringsberg (2020). In this method, the coefficients are calculated based on results from Da-Qing et al. (2012) and the spin ratio, SR. This method is chosen as a result of being valid for larger intervals of SR. The spin ratio is defined as the ratio between the rotor's tangential speed and the local apparent wind speed, where the recommended spin range is between 1 and 3. The lift coefficient C_L, drag coefficient C_D and power coefficient C_P can then be derived as in respectively Equation 6.2, Equation 6.2 and Equation 6.4.

$$C_L = -0.0046SR^5 + 0.1145SR^4 - 0.9817SR^3 + 3.1309SR^2 - 0.1039SR \tag{6.2}$$

$$C_D = -0.0017SR^5 + 0.0464SR^4 - 0.4424SR^3 + 1.7243SR^2 - 1.641SR + 0.6375 \tag{6.3}$$

$$C_P = 0.0001SR^5 - 0.0004SR^4 + 0.0143SR^3 - 0.0168SR^2 + 0.0234SR \quad (6.4)$$

When calculating wind shear, or wind speed profile, the Hellman coefficient is set to 0.14, which is used for offshore wind turbines and is assumed to have similar wind conditions as to vessels operating in deep-sea shipping. Since the apparent wind angle (AWA) and speed (AWS) vary over the height above the sea, the Flettner rotor is divided into horizontal strips, where the thrust, side force and power are calculated for each strip. The total aerodynamic thrust, side force and power required for spinning each rotor can then be found by summation over all the strips. If the required power for spinning the rotor is larger than 10% of the installed power, the case is set as feasible to ensure the motor is not overpowered.

By assuming 10% in electrical losses between the diesel generator and the electrical motor for spinning the rotor, the required power for the WASP is found. Then the total amount of power that must be provided to the ship, including propellers, are calculated. The required power derivatives are multiplied by the ship speed and the cosine of the drift angle to account for the fact that the ship speed and surge speed are not the same due to drift. By subtracting the effective thrust difference from WASP divided by 0.6 to account for propeller efficiency, the required power for the propellers is found. The saved power can now be found by subtracting the required power from the rotors and propellers for the baseline required power. Required baseline power is determined by the third degree polynomial in Figure 6.2a, describing the vessel power consumption as a function of ship speed, when the vessel experience no drift.

The output from the Matlab code is drift angle, constraint limit, effective thrust from the rotors, side force, required power, saved power, savings in percent and fuel saved as a function of ship speed, true wind speed and true wind angle. If the outputs are set to 0, the code could not find a solution based on a constraint limit. There are a total of 8 constraint limits:

1. Too high wind speed, regardless of wind angle.
2. All possible rotor RPMs were tried and the limit for maximum rpm was reached.
3. All possible rotor RPMs were tried and the limit for maximum spin ratio was reached.
4. Too high required power for the Flettner rotor.
5. Too large side force on the hull.
6. Too large thrust on the Flettner rotor.
7. Too large side force on the Flettner rotor.
8. Too large electric motor is installed in the Flettner rotor.

The outputs from the code can then be plotted as a function of ship speed, true wind angle and true wind speed. Furthermore, the results presented as a function of the wind angle are based on the true wind angle and speed, since the apparent wind angle and speed vary by the height above sea level.

At last, it is important to acknowledge the limitations of the code. By not having rudder included in the code, one assumes that yaw moment will not make the ship go into circles. In reality, there is added resistance due to the rudder angle compensating for the yaw moment. Moreover, the location for the Flettner rotors is not included. The placement of the rotors will affect interaction effects from bound vortex, yaw moment, the rudder angle and corresponding increased resistance. Finally, increased drag from headwind and increased thrust from tailwind are neglected. The thrust or drag at these wind conditions will not be correct, however, it is assumed to be a valid assumption when investigating the wind conditions throughout one year.

6.5 Combining weather data and effects of WASP

After obtaining the weather data for the specific route and a general estimation of the effects of WASP, these data must be combined to estimate the effects of WASP on the specific route. The code does this in Section B. For every data point in the vessel sailing and weather data, the row in the Matlab output file corresponding to the ship speed, true wind angle and true wind speed is found using the defined *WASP output* function in Section D. From this row, values such as effective rotor power, savings in percent, and fuel savings are extracted and saved as a CSV file for further analysis. Based on the routes sailed throughout the year, savings for each route is calculated and presented as histograms and colorized on a map format by using the defined function *linePlottingColorsPercent* in Section D.

6.6 Operational modes

As described in Section 3.2, there is potential for saving fuel consumption by adapting the operational pattern of a vessel fitted with WASP. In this case, the fixed time operational mode is applied to the base case by using the code in Section C. Firstly, the data is divided into groups for each voyage to avoid including time in port. The code then iterates through every data point for each voyage to find a new speed profile matching the time used on the original sailing. If there are no contributions from the wind, the ship speed is set to 10 knots. Based on the power generated from the wind, the ship's speed is increased accordingly up to 20 knots. If the new sailing time for the voyage is off, the ship speeds are changed by an increment of 0.25 knots. This iteration is repeated until the difference between the new and old sailing time are within a set interval. Additionally, the code ensures that the vessel does not exceed it's maximum velocity.

At last, the fixed power operational mode is used to estimate savings. This is done by creating a new function for finding the WASP outputs called *WASP output fixed*

power in Section D. Instead of finding the outputs based on wind direction, wind speed and ship speed, the code finds the corresponding row based on wind direction, wind speed and the engine power. As a result, ship speed is one of the outputs and the average sailing speed for a range of fixed engine powers can be estimated.

6.7 Validation of the results

At last, the results are validated to obtain a measure of the accuracy of the model. To validate the potential savings found in the results, the Energy Technology Institute's Flettner Rotor System Tool will be used. The tool was developed by Lloyd's Register's Ship Performance Group by using in-service data collected from the Maersk Pelican (Now Timberwolf) together with well-known ship performance calculation methods, average global wind statistics and aerodynamic coefficients of generic merchant ship types. The tool is generalized and can be used for different vessel types, Flettner rotor configurations, loading conditions, sailing speeds and trading routes. The outputs of the model are a plot of savings against the distance, a performance polar plot which displays the fuel savings depending on wind speed and wind angle, and at last, a table of monthly savings in propulsion consumption and emissions (Lloyd's Register Advisory Services BV 2020).

6.8 Summary of the method

To give an overview of the steps needed to be taken for a ship owner to perform a similar study, the method can be summarized as a "step-by-step" approach as followed:

1. Decide on which vessel is appropriate for WASP retrofit and determine Flettner rotor configuration based on vessel size and available deck area.
2. Set an interval of the operation that is relevant for future operations and obtain the AIS data.
3. Obtain metocean hindcast data based on the corresponding AIS data and a set time step.
4. Calculate Flettner rotor performance for all combinations of true wind speed, true wind angle and ship speed.
5. Estimate the performance of the vessel by combining the weather data and Flettner rotor performance.

Chapter 7

Results

This chapter presents all the results derived from the method used and data collected in previous chapters. The results and corresponding figures give an indication of the feasibility of a potential WASP conversion for the vessel, in addition to illustrating some of the necessary results and assessments needed to be taken by a shipowner considering a similar conversion for a vessel or fleet.

7.1 Base case

The vessel data can now be analyzed. In Table 7.1 and Figure 7.1, the routes sailed by the vessel throughout the course of one year are displayed. The vessel berths at a total of 17 ports/terminals and covers a total distance of 103 078 nautical miles. The average speed of the vessel is 16.5 knots whereas the vessel has mostly operated between 14 and 20 knots as shown in Figure 7.2. The data that is being used represents the vessel's operation throughout the course of one year and consists of 206 000 registrations, which corresponds to an average registration rate of every 2 minutes and 33 seconds.

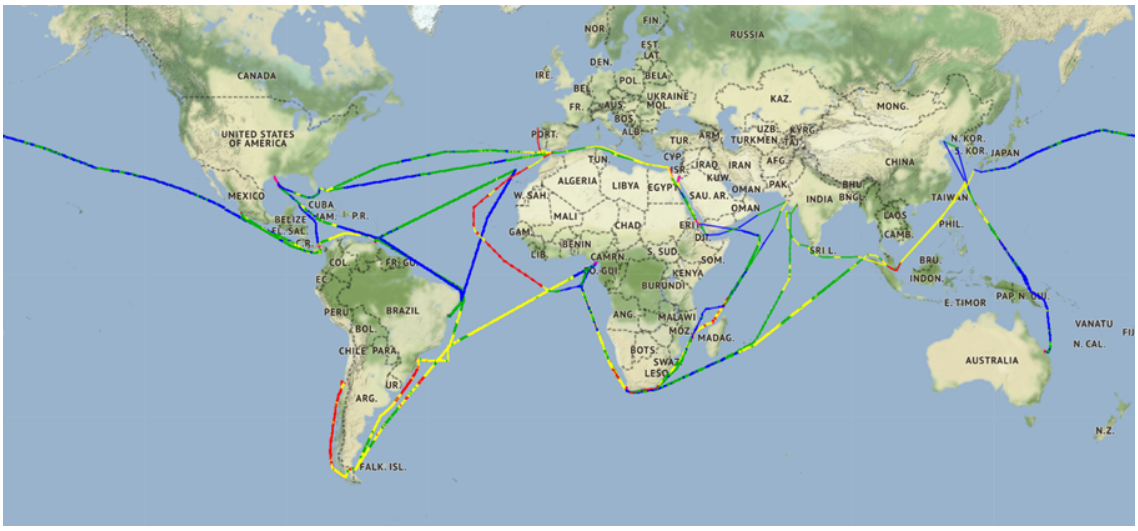

Figure 7.1: Vessel routes; >18 knots (blue), 16-18 knots (green), 14-16 knots (yellow), 10-14 knots (red), <10 knots (pink)

Table 7.1: Routes for case study

Port of departure	Sailing time to next port [days]	Sailing distance [nm]	Average sailing speed [knots]
Port of Caofeidian, China	16	4402	16.3
Port of Gladstone, Australia	36	8788	18.1
Dahej port, India	22	7629	16.9
Malabo, Equatorial Guinea	34	10460	16.6
Port of Caofeidian, China	31	10416	18.0
Louisiana, USA	24	7375	17.7
Port of Aqaba, Jordan	30	10385	15.5
Malabo, Equatorial Guinea	24	8075	14.9
Viña del Mar, Chile	30	7070	15.5
Point Fortin, Trinidad & Tobago	19	3024	14.9
Manzanillo, Mexico	10	3188	16.2
Point Fortin, Trinidad & Tobago	14	5847	18.3
Salvador, Brazil	13	4714	19.2
Louisiana, USA	27	9700	17.3
Mundra, Gujarat, India	20	7408	17.0
Malabo, Equatorial Guinea	16	5013	14.5
Gibraltar, Spain			

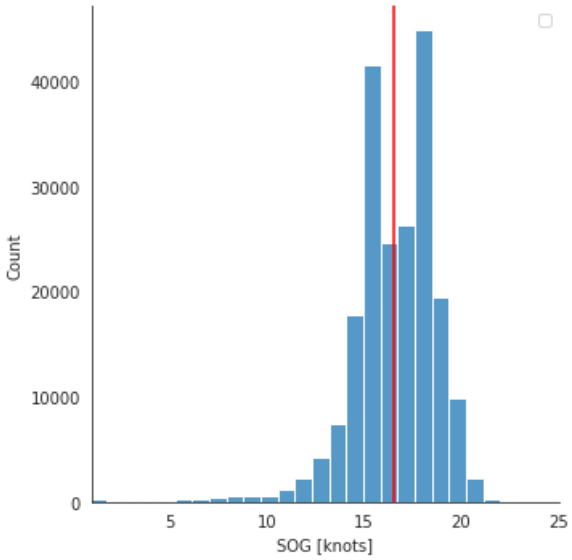

Figure 7.2: Vessel speed profile with speed over ground in knots with average speed (red)

The distribution of true wind speed and true wind angle is found in Figure 7.3. The figure displays an under-representation of tailwinds and a slight bias of wind from at 45°and 270°. The registered wind speeds are mostly below 10 m/s as shown by the green and blue colors.

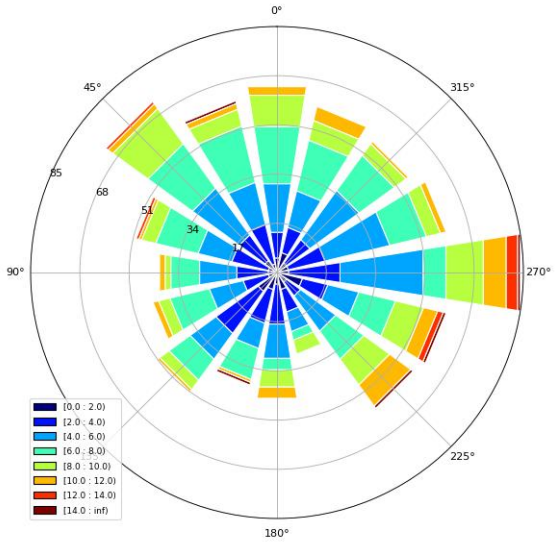

Figure 7.3: Windrose plot of true wind speed and true wind angle

The distribution of wind speeds can be found in Figure 7.4. Average wind speed is found to be 5.1 m/s indicated by the red line. The average of the 90% highest wind speeds was found to be 9.0 m/s which is indicated by the yellow line.

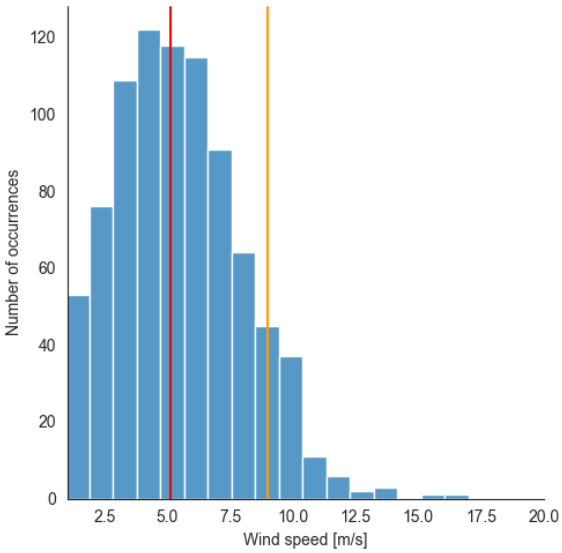

Figure 7.4: Distribution of wind speeds experienced by the vessel

7.2 Fuel savings

The output of fuel savings from the Matlab code is presented in Figure 7.5 for a ship speed of 16.5 knots. It presents fuel savings in percent as a function of true wind angle and true wind speeds between 0 and 20 m/s. The figure shows that the vessel can save fuel with a true wind angle between 20°and 160°for wind speeds below 10 m/s. The savings increase for higher wind speeds, however, the vessel is not able to generate thrust for the same tailwind angles. The reason for not being able to generate lift at these particular angles will be explained in Section 7.6. As shown by the color scale, the Flettner rotor configuration is able to save power equivalent to up to 84% compared to the baseline fuel consumption. These savings are achieved at high wind speeds at TWA of around 120°and 240°

In Section E, the same polar plot is displayed from vessel speeds between 8 and 22 knots, which covers the vessel speed profile. At low ship speeds, the vessel generates a high reduction in fuel consumption up to 100% over a shorter interval of true wind angles. With an increase in ship speed, fuel consumption is achieved over a larger interval of true wind angles and the savings show a clear decreasing tendency in percent.

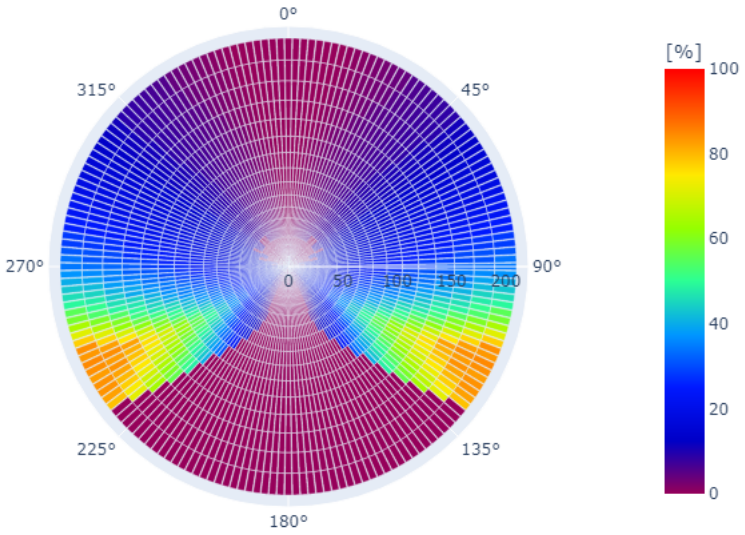

Figure 7.5: Percent of fuel saved as a function of true wind angle and true wind speed [m/s] at vessel speed of 16.5 knots

By combining the results obtained from the experienced weather and the output from the Matlab code, fuel savings for the base case are calculated. The average fuel savings is found to be 4.5% and the average of the 10% highest registered savings is 12.3%, which are presented as vertical lines in respectively red and yellow in Figure 7.6. The figure also shows a high representation of registered low savings where the vessel experience 0% savings, 41.0% of the time.

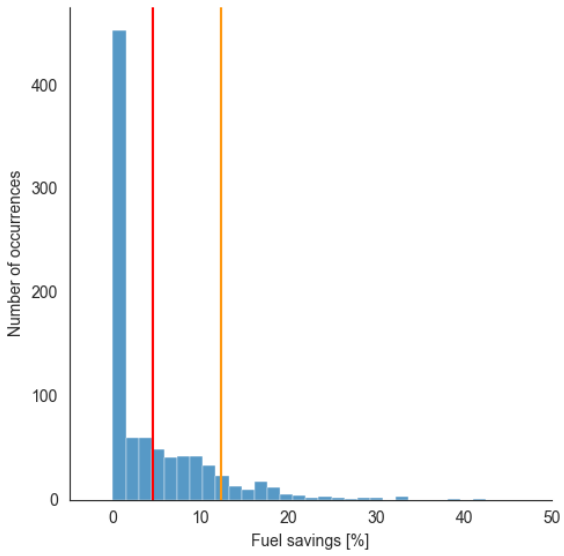

Figure 7.6: Distribution of fuel savings throughout one year with average (red) and average of the highest 90% (yellow)

In Figure 7.7a and Figure 7.7b, the fuel savings for each individual route is presented with the overall average displayed as a horizontal red line where the average of 4.5% fuel savings corresponds to 127 kg/h. The routes with the largest percentile savings are route number 1, 7, 12 and 16 which are the sailings between China and Australia, Jordan and Equatorial Guinea, Trinidad & Tobago and Brazil, and Equatorial Guinea and Spain. Regarding the absolute savings, voyage number 12 has the highest average savings with close to 250 kg/h. In Figure 7.8, these routes together with the vessels' operation throughout the year is plotted on a map with the color corresponding to the fuel savings.

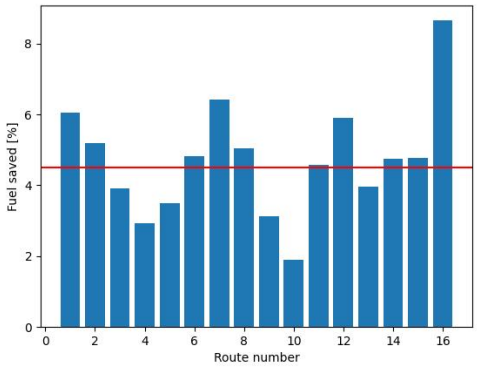

(a) Average percent power saved for each route with overall average (red)

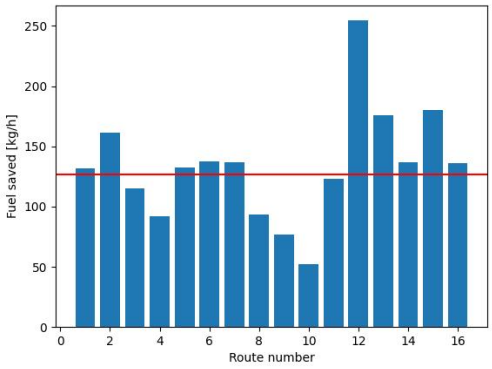

(b) Average fuel saved for each route with total average (red)

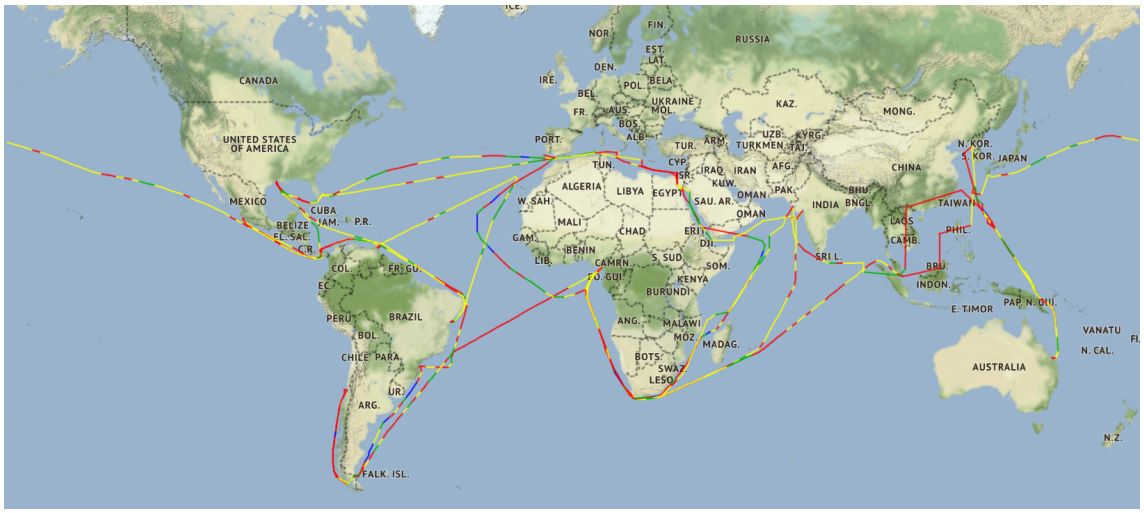

Figure 7.8: Vessel route with fuel savings; >20% (blue), 20%-10% (green), >0%-10% (yellow), 0% (red)

7.3 Effective thrust

The maximum thrust generated by the Flettner rotors combined is displayed in Figure 7.9 as a function of true wind angle at a vessel speed of 16.5 knots for all

true wind speeds. The configuration has potential of generating effective thrust exceeding 878 kN for true wind angles between 110°-130°and 230°-250°, which is at high wind speeds close to 20 m/s. In Section F the same figure is presented for vessel speeds between 8 to 22 knots. At low sailing speeds, thrust exceeding 800 kN is generated, however, this is for a small interval of wind angles between 110°and 120°, and corresponding wind angles at port side. For higher vessel speeds up to 22 knots, the maximum thrust exceeding 800 kN is produced between 105°to 135°.

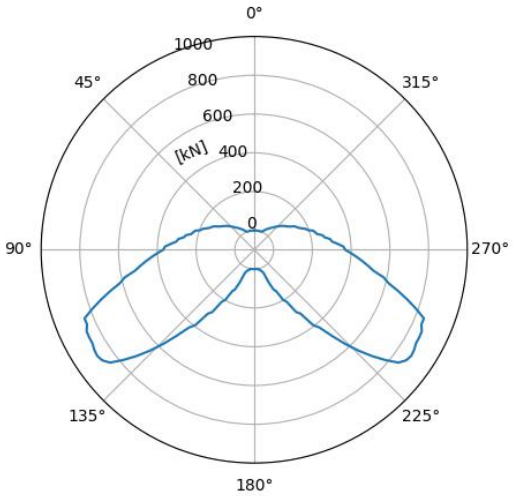

Figure 7.9: Effective thrust at 16.5 knots

7.4 Effective rotor power

The maximum effective rotor power for all true wind speeds and vessel speed of 16.5 knots, as a function of true wind angle is shown in Figure 7.10. For the same true wind angles as in Section 7.3, the Flettner rotors are able to generate up to 7063 kW. In Section G, the maximum effective rotor power is presented for ship speeds between 8 to 22 knots. The predominant amount of effective power is achieved at true wind angles close to 110°and 250°for low ship speeds. At low ship speeds, the highest effective power generated is close to 3500 kW. At higher ship speeds, the rotors generate higher effective power at an increasingly larger range of wind angles. The maximum effective power of 9150 kW is generated with a vessel speed of 22 knots and high wind speeds, close to 20 m/s.

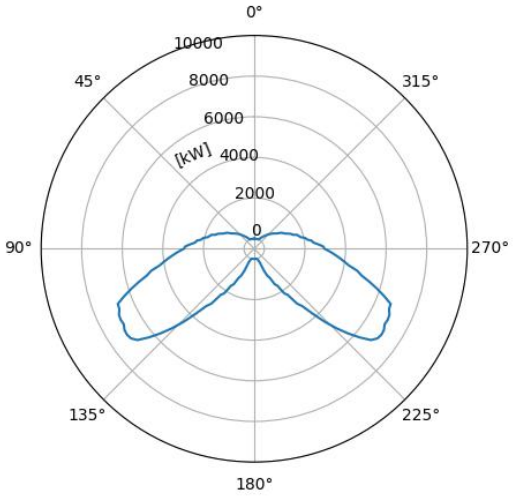

Figure 7.10: Effective power at 16.5 knots

7.5 Costs

To assess the economic viability of the project, it is necessary to calculate the discounted payback period for the investment. Since this investment is of a climate friendly character, the discount rate is set low, to 5%. By using the fuel prices presented in Section 3.3, the discounted payback period can be derived as shown in Figure 7.11. For the low fuel cost, medium fuel cost and high fuel cost, the payback periods are respectively 23.1 years, 7.2 years and 3.0 years. The balance of the project after 25 years is respectively 0.1M USD, 5.1M USD and 14.7M USD.

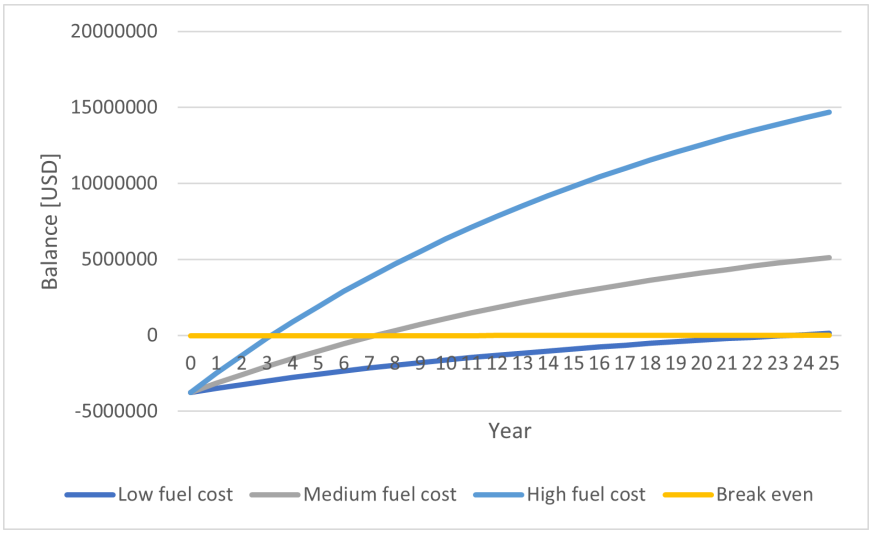

Figure 7.11: Discounted payback period for five 4x24m Flettner rotors

7.6 Constraint limits

As mentioned in Section 6.4, the code outputs a constraint limit when the given conditions do not generate a reduction in power consumption. In Figure 7.12, the colors express the different constraint limits as a function of true wind angle and true wind speed for a ship speed of 16.5 knots. The dominating constraint limits are 2, 3 and 5, in addition to 0 (blue) which corresponds to beneficial wind conditions that generate thrust. Regarding constraint limit 5 (yellow), headwind and tailwind contribute to a too large side force on the hull. In practice, this means that the rotors must be switched off and will be creating drag. For tailwind, constraint 2 (light blue) is one of the dominating limits. In these conditions, the code is not able to find a suitable rotor RPM within the given boundaries since the maximum rotor RPM was set too low. When the vessel experience tailwind close to 180°at low wind speeds, constraint limit 3 (light green) is reached. In this case, the maximum spin ratio was too low for the rotors to generate thrust at these low wind speeds.

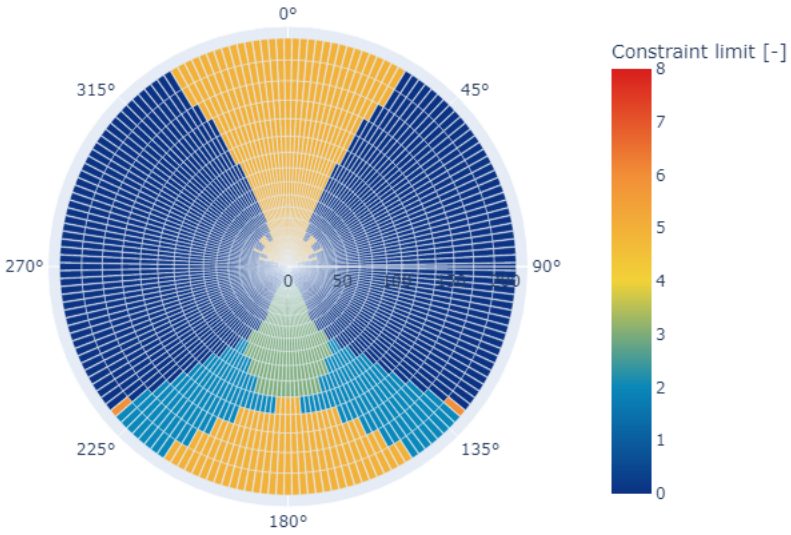

Figure 7.12: Constraint limit as a function of true wind angle and true wind speed [m/s] at vessel speed of 16.5 knots

The constraint limits experienced by the vessel for one year of operation is presented in Figure 7.13. Constraint limit number 5 is the limit that occurs most often, followed by constraint limit number 3.

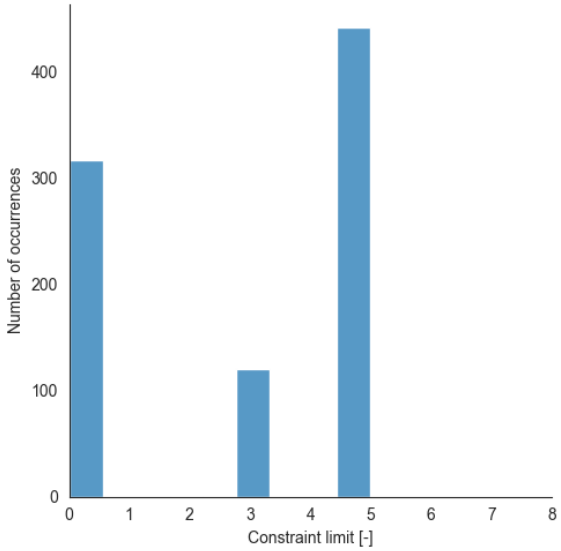

Figure 7.13: Constraint limits experienced by the vessel

7.7 Concepts of operation

In the previous sections, the results have been derived based on an operational mode for a vessel without WASP. As explained in Section 3.2, fuel savings can be further increased by adapting the operational mode to the weather conditions and in particular the thrust generated from the sails. In this section, the results from applying the fixed time and fixed speed operational mode is presented.

By introducing slack in the sailing time of maximum 6 hours, the average sailing speed is reduced to 14.4 knots as displayed by the red line in Figure 7.14. The speed profile is more distributed along the range of 8 to 22 knots with some clusters around 9, 12, 15 and 22 knots due to reoccurring wind conditions. As a result of adapting the sailing speed to a fixed operational time, the fuel savings are increased from 127 to 206 kg fuel per hour. It is important to emphasize that this increase in fuel savings is a result of increasing the vessel speed as a function of favorable wind conditions. However, the average speed is reduced which brings the average fuel consumption from 2496 to 1935 kg/h. This reduction corresponds to 22.5%.

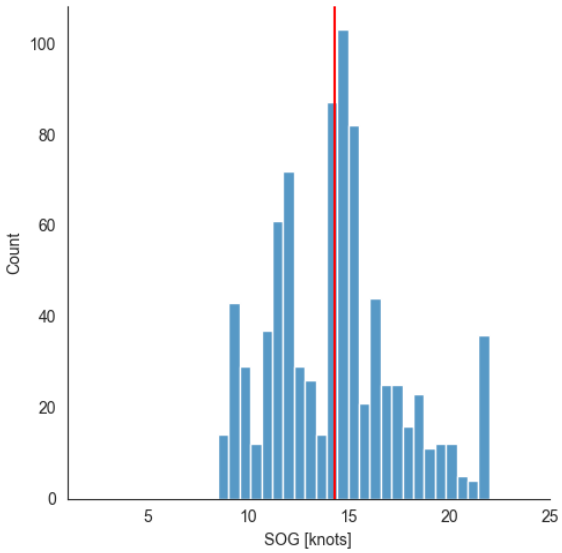

Figure 7.14: Vessel speed profile with speed over ground in knots and average speed (red)

Average fuel consumption and ship speed are now estimated for fixed power operational modes. In Table 7.2, the results from the vessel sailing through the waypoints from the AIS data with fixed power between 2000 kW and 26 000 kW, are presented. The speed ranges between 10.2 to 20.0 knots and both the fuel consumption and fuel saved due to the Flettner rotors, increase with higher power consumption.

Table 7.2: Fuel consumption vs. fixed power

Fixed power $[kW]$	Avg. ship speed $[knots]$	Avg. fuel saved $[kg/h]$	Avg. fuel consumption $[kg/h]$
2 000	10.2	28	681
4 000	12.2	40	1051
6 000	13.7	54	1433
8 000	14.7	71	1749
10 000	15.5	91	2033
12 000	16.3	116	2327
14 000	17.1	148	2622
16 000	17.7	179	2899
18 000	18.2	204	3204
20 000	18.8	244	3570
22 000	19.1	274	3812
24 000	19.6	321	4155
26 000	20.0	380	4567

7.8 Validation of the obtained results

The performance polar plot from the output of Loyd's Register Flettner rotor savings estimator is presented in Figure 7.15a. The vessel particulars are similar to the base case vessel and the ship speed is set to 16.5 knots. The plot displays a percental saving exceeding 20% with true wind speeds above 10 knots within wind angles between 85°-155°and 205°-27°. When experiencing tailwind, the vessel is able to generate thrust between 0% and 5%. For headwind, the savings are between -5% to 0% for true wind angles between 30°and 330°. At 16.5 knots, the program estimates that fuel savings in global wind conditions are 3.0%. In Figure 7.15b, the results from the Matlab code are plotted with colors corresponding to the plot from the Flettner rotor savings estimator. The two plots show similar results for headwind, however, there are some discrepancies that will be further discussed in Chapter 8.

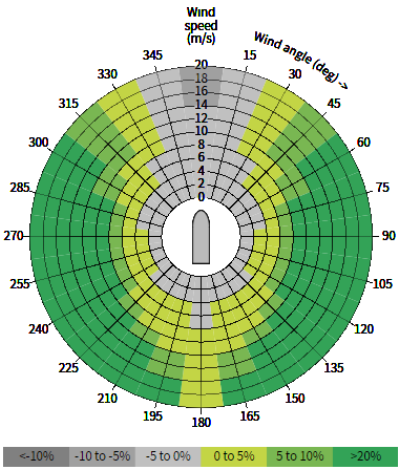

(a) Performance polar plot, Loyd's Register Flettner rotor savings estimator

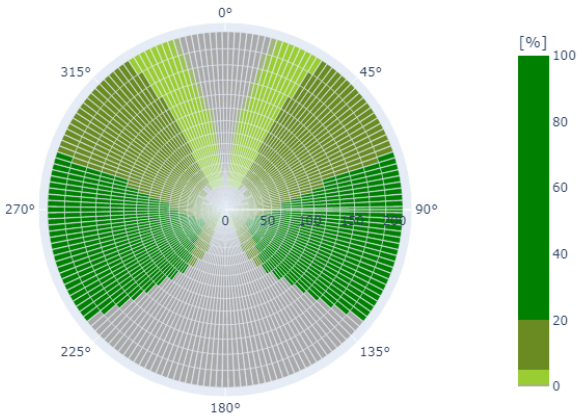

(b) Performance polar plot, Matlab code

Chapter 8

Discussion

8.1 WASP concepts

In the literature study, five different WASP technologies were investigated. It is clear that Flettner rotors have received the broadest reception from relevant stakeholders. The technology has been in operation for many years, its performance is well documented and the manufacturers are also well established. At low wind speeds, it creates a lot of drag, however, it can also generate a lot of lift due to its high lift coefficient. Additionally, it is also versatile in terms of generating lift from different wind directions. Its success can be traced back to that the implications on the systems and operations on the rest of the ship are low. For an operator, the system is relatively easy to handle as it only requires adjustment on RPM. The system also requires less deck space due to its high lift coefficient so that loading and offloading become easier to handle with the Flettner rotor.

Other WASP concepts included were the wing sail, towing kite, suction wing and soft sails. Comparing the Flettner rotor with the Dynarig (soft sail) and wingsail, they all show promising results in terms of fuel savings. As shown in Figure 5.4, the Dynarig and wingsails show similar results with savings above 20% with strong cross winds and lower sailing speeds (Reche-Vilanova et al. 2021). It therefore remains to answer why there are only one wingsail and zero soft sail installations of these systems within commercial shipping. It might be the tradeoff between fuel savings and how it affects the ship's logistics and operation. These systems have a lower lift coefficient than the Flettner rotor, requiring more sail area for the same amount of thrust. Larger sails have major implications on especially loading operations on vessels that are loaded through the main deck. In addition, the systems' operations are more complex than adjusting the RPM on the Flettner rotor. Although the concepts have existed for a long time, the technology maturity within modern commercial shipping is lacking.

On the other hand, the towing kite and suction wing are concepts that are more tested within commercial shipping. Five vessels are sailing with a towing kite and two vessels are fitted with suction wings. Comparing them to the other WASP systems, there are far less available research on the topic. For industry stakeholders

considering which technology to invest in and use for its fleet, it is less likely to land on less proven technology. Additionally, it is worth questioning why there has not been installed a towing kite since 2012. As mentioned, the RO-RO vessel Ville de Bordeaux is planned to install a towing kite. However, it is also worth questioning why the only vessel that will be equipped with a towing kite over the last ten years is leased to Airbus on a 20+10 year contract, and the supplier of the towing kite is owned by Airbus.

8.2 Method

To evaluate how the method performs, it is necessary to discuss to what extent this method is applicable to a ship owner. Essential assessment criteria are if the estimates are accurate enough and user-friendliness such as short running times, and if all necessary data is available.

Regarding user-friendliness, the calculations of parameters such as saved fuel can be derived for further economic analysis in a few hours. Additionally, the method only requires AIS data and vessel main particulars, which are easily accessible to a ship owner. However, this method requires that one is experienced with programming, both within Matlab and Python. The method used is performed in several steps, where each stage allows for an additional source of error in terms of inputs and potential troubleshooting. As a result, it might be beneficial for this method to become more streamlined such as a program where the user operates on a higher level of coding than as performed in this thesis. On the other side, constructing such a program could be too time-consuming for a ship owner, and it might be more appropriate for stakeholders providing similar services to ship owners to create such a program. If such a program were to be constructed, one could argue that the model should compare several configurations of Flettner rotors, since that will become more time consuming with the existing method.

The method makes several simplifications that can decrease the accuracy of the results. Firstly, wave data is neglected in the calculations. In reality, there will be increased resistance due to waves when there are favorable wind conditions for the Flettner rotor, and the estimates might be too optimistic. Furthermore, the weather data used is only available for dates up to 2020, which can be problematic if the ship owner wishes to evaluate the WASP potential for recent operations. There are two workarounds for this problem whereas the first one is to use metocean hindcast databases with less geographical coverage and more recent data. Secondly, one can utilize weather distributions based on location and time of year. Additionally, the vessel could have used weather routing. Hence, the waypoints from the AIS data can be less optimal for generating lift from the Flettner rotors. In that case, AIS data would not be the preferred method for determining waypoints. Whether this is the case will be easier to evaluate for a ship owner who has more knowledge about the vessel's operation. It is worth mentioning that a form of reversed weather routing might be applicable for determining routes that encounter wind conditions that are more beneficial for a WASP vessel.

The final assumptions used when calculating the contributions from the Flettner rotors are increased drag and weight from the rotors and viscous interaction effects between the rotors themselves. Increased drag due to a more exposed area on the deck will have an effect on a short-term perspective, however, for a whole year of sailing, it is assumed to be a valid assumption since headwind and tailwind conditions are likely to be equally distributed. From the wind rose plot in Figure 7.3, this is confirmed. The reduction in DWT due to the increased weight of five Flettner rotors is 215 tonnes, which is small compared to the total DWT of 83 600. However, it should be included for more accurate economic estimates. Regarding the neglection of the viscous interaction effects of airflow between the rotors, it cannot be included when the placement of the rotors is not included in the code. Together with the assumptions mentioned above, how valid this assumption is will have to be discussed using the accuracy of the results derived from the case study.

8.3 Results

The results from the case study form the basis of the evaluation of determining the potential for retrofitting Flettner rotors on the particular vessel. The vessel used in this case study has an operational profile with high sailing speeds compared to other ships. At these sailing speeds, the fuel consumption is high, however, the effective power from thrust produced by the Flettner rotors is also high. Hence, the total fuel savings are more significant at higher sailing speeds. Since the vessels sails on a range of different sailing routes with varying sailing speeds, this can be seen in the histograms of the fuel savings by routes, in Figure 7.7a and Figure 7.7b. Some exceptions can be explained by varying wind conditions, however, the voyages with high fuel savings in percent have low average sailing speeds, and the ones with more considerable fuel savings in kg/h are the ones with higher sailing speeds.

The same observations can be made for the polar plots. The polar plots for savings in percent show that the percentile savings increase when decreasing the ship speed. In theory, it is possible to generate more than 100% of the power needed for powering the vessel, which occurs when the required power to the propellers is negative. In practice, this would correlate to an increase in sailing speed. However, if the vessel were equipped with a hybrid-electric propulsion system, one could generate power to a battery by using the propellers to retard the ship. Looking at the plots from the effective thrust, the maximum thrust generated is similar for all vessel speeds. These findings are in line with Reche-Vilanova et al. (2021), where it was found that the performance of the WASP device is similar for varying sailing speeds, however, the absolute savings increase with higher sailing speeds.

The constraints show that the Flettner rotors cannot generate lift at wind angles close to tailwind and headwind conditions. Under these conditions, the lift will act perpendicular to the vessel heading, and the vessel is not able to generate thrust. This constraint will dominate for a larger interval of wind angles when the wind strength increase due to the rise in both lift and drag, which is in line with the observations from the polar plots. Since the hydrodynamic lift coefficient for the hull increase with higher ship speed, the vessel can withstand more side force. This is

in line with the observations found in Figure 1, where too much side force is created at low ship speeds. Other predominant constraint limits are too large spin ratio and too large RPM required. In practice, these are the same thing, however, they are separated for research measures. If the required RPM is too high, the bottleneck is the Flettner rotor supplier, where there is a need for motor and bearing withstanding higher RPMs. For too large spin ratio required, there is a need for more research at higher SRs to investigate what the lift and drag coefficients are at these spin ratios. By increasing the allowable RPM, the required power to the Flettner rotors will increase, however, the rotor will be able to generate lift at more wind angles and potentially reduce fuel consumption, as found in Lu and J. Ringsberg (2020). The results from the case study in Figure 7.13, show that the constraint limit for the max spin ratio was the second most reoccurring limit. Hence, increasing the maximum spin ratio would have reduced fuel consumption.

Since the polar plots are plotted as a function of true wind angle, the visualization can appear misguiding. When the vessel speed increase, the apparent wind angles become more tail biased. Hence, more side force is created, and the rotors cannot generate thrust at a larger interval of true wind angles. As mentioned, the results were presented in this manner due to the outputs of code being true wind angle and that the apparent wind angle varies as a function of height above the sea level. This can explain the difference in the polar plot obtained from the Matlab code and the one from Loyd's Register Flettner rotor savings estimator in Section 7.8. If the results were plotted by apparent wind direction, the plot would show that the Flettner rotor can generate thrust at more tailwind angles, similar to the one from Loyd's. Considering the difference between true wind angle and apparent wind angle, the figures show similar fuel savings for the same wind speeds and angles. On the other side, the estimator presents that the fuel savings in global wind conditions are 3.0%, which is 50% higher than estimated by the method in this thesis. Some discrepancies can be justified due to variation in wind conditions, however, some of the divergences might be to the method overestimates the fuel savings. Further validation on the model will therefore have to performed. If the results were of sufficient accuracy, the economic analysis shows that the vessel has potential for a more thorough analysis for a potential retrofit of Flettner rotors.

Finally, the fuel savings are estimated for fixed time and power operations. The average speed is reduced by 2.1 knots for the fixed-time operations. Some of the reduction can be explained by introducing soft time windows for every arrival to ensure that the code would iterate to a valid solution. However, when analyzing the AIS data, it appeared that the vessel could be moored by anchor or steaming in circles for up to two days before berthing for offload/unload. From the speed profile in Figure 7.2, there are few registered speeds below 7 knots, and one could presume that data entries are missing. Hence, the actual average speed might be less than 16.5 knots. The speed reduction mainly causes the average fuel consumption, which is reduced by 561 kg/h. However 79 kg/h of the reduction can be traced back to the effect of sailing faster when experiencing beneficial wind conditions. With fixed power operational mode between 2000 kW and 26 000 kW, there is also a substantial increase in fuel saved and consumed when increasing the fixed power. However, the most important finding is that the vessel can obtain high average sailing speeds

despite great reduction in available power. By halving the available power from 24 000 kW to 12 000 kW, the average speed is only reduced from 19.6 knots to 16.3 knots, close to the original operation's average speed. At 2000 kW, which is 6.3% of installed power, the vessel can maintain an average speed of 10.2, which is close to the speeds found in Woodward et al. (1975) and Perez et al. (2021) for the vessels sailing at 6 knots at less favorable wind conditions.

Chapter 9

Concluding remarks

In the literature study of this report, it is found that among the Flettner rotor, wingsail, soft sail, towing kite and suction wing, the Flettner rotor appears to be the most promising solution for wind assisted ship propulsion. To conclude what has been stated so far, the technology is gaining ground due to three reasons. The systems are relatively easy to operate as it only requires RPM adjustment. Secondly, it has a low effect on surrounding systems and the logistics due to its high lift coefficient. Finally, the technology has been tested for many years, resulting in well-documented effects, much research on the topic, and established suppliers.

The method used in this thesis only requires available data and the calculations made are not time-consuming from a computational point of view. Although the process has the potential to become more streamlined, it is concluded that the method fits as a preliminary method for evaluating the potential fuel savings from a Flettner rotors vessel in an early stage design process.

The results derived from the method show that the vessel used in the case study has the potential for retrofitting five 4x24m Flettner rotors from an economic point of view. It is found that the vessel can save 4.5% of its actual fuel consumption by sailing with the same operational profile. Using the average fuel price from the last two years, which is conservative by today's standard, the investment will be paid back by 7.2 years if the discount rate is set to 5%.

By introducing fixed time and fixed power operational modes, further fuel consumption reductions can be made by adapting the sailing speed based on the wind conditions. Increasing the sailing speed when experiencing beneficial wind conditions will increase the total savings. More specifically, it was found that the average savings from wind propulsion can be increased by 80 kg/h for the case study by introducing a fixed time schedule. Additionally, the required power for maintaining the same average sailing speeds is notably decreased when introducing WASP.

9.1 Further Work

A natural course for further work is a development of the model. Firstly, the method could be validated by applying the method on vessels fitted with Flettner rotors and comparing the results to the actual reported savings. Secondly, the model has potential to become more user-friendly by integrating it into a software. Additionally, the Matlab code has to be run for every alteration of the inputs, and for a method used in early-stage design, it is necessary to test the performance of different Flettner rotor configurations. Therefore, the code could be implemented into an optimization algorithm that can identify the optimal configuration, including number of rotors, size, and placement. One could also investigate the potential for using weather routing to plan routes with beneficial wind conditions to further increase fuel consumption. At last, a risk assessment of WASP vessels could be performed since it is demanded by the class society to achieve the additional WAPS class notation.

Bibliography

Airseas (2021). *Seawing*. URL: https://www.airseas.com/seawing (visited on 15th Dec. 2021).

Ariffin, N and Mohammed Abdul Hannan (June 2020). 'Wingsail technology as a sustainable alternative to fossil fuel'. In: *IOP Conference Series: Materials Science and Engineering* 788, p. 012062. DOI: 10.1088/1757-899X/788/1/012062.

Ashmore, Jehan (Mar. 2022). *North Sea Region Adds a New Wind-Assist Rotor Installed Vessel to the Fleet*. URL: https://www.maritime-executive.com/article/rotor-sails-to-be-fitted-to-largest-short-sea-ro-ro (visited on 30th May 2022).

Blueburd Marine Systems (2021). *Monorotor - Wind Assisted Propulsion*. URL: https://www.bluebird-electric.net/ship_boat_design_building/monorotor_wind_assisted_ship_propulsion.htm (visited on 15th Dec. 2021).

Brouwer, Jacqueline (May 2021). *North Sea Region Adds a New Wind-Assist Rotor Installed Vessel to the Fleet*. URL: https://northsearegion.eu/wasp/news/north-sea-region-adds-a-new-wind-assist-rotor-installed-vessel-to-the-fleet/ (visited on 30th May 2022).

Chambers, Sam (Feb. 2020). *Dutch pioneering wind technology makes debut trip across the North Sea*. URL: https://splash247.com/dutch-pioneering-wind-technology-makes-debut-trip-across-the-north-sea/ (visited on 9th Dec. 2021).

Chou, Todd et al. (Feb. 2021). 'A Comeback of Wind Power in Shipping: An Economic and Operational Review on the Wind-Assisted Ship Propulsion Technology'. In: *Sustainability* 13, p. 1880. DOI: 10.3390/su13041880.

Conoship (2021). *Econowind-unit*. URL: https://www.conoship.com/portfolio-item/econowind-unit/ (visited on 9th Dec. 2021).

Wind assisted propulsion systems (Nov. 2019). Standard. DNV. URL: https://rules.dnv.com/docs/pdf/DNV/st/2019-11/dnvgl-st-0511.pdf.

Dykstra naval architects (2021). *WASP (Ecoliner)*. URL: https://www.dykstra-na.nl/designs/wasp-ecoliner/ (visited on 9th Dec. 2021).

E.U. Copernicus Marine Service Information (2021). *Global Ocean Wind L4 Reprocessed 6 hourly Observations*. Data retrieved from: https://doi.org/10.48670/moi-00185.

Epifanov, V. M. (Feb. 2011). *Suction effects*. URL: https://thermopedia.com/content/1166/ (visited on 9th Dec. 2021).

IMO (2020). *Fourth Greenhouse Gas Study 2020*. URL: https://www.imo.org/en/OurWork/Environment/Pages/Fourth-IMO-Greenhouse-Gas-Study-2020.aspx (visited on 12th Dec. 2021).

Joung, Tae-Hwan et al. (Jan. 2020). 'The IMO initial strategy for reducing Greenhouse Gas(GHG) emissions, and its follow-up actions towards 2050'. In: *Journal of International Maritime Safety, Environmental Affairs, and Shipping* 4, pp. 1–7. DOI: 10.1080/25725084.2019.1707938.

Kaltschmitt, Martin, Streicher Streicher Wolfgang and A. Wiese (Jan. 2007). *Renewable energy: Technology, and environment economics*, pp. 1–564. DOI: 10.1007/3-540-70949-5.

Kawasaki (Dec. 2019). *Delivery of LNG Transport Vessel MARVEL PELICAN*. URL: https://global.kawasaki.com/en/corp/newsroom/news/detail/?f=20191213_6735 (visited on 29th Apr. 2022).

Kijima, Katsuro et al. (1990). 'On the manoeuvring performance of a ship with theparameter of loading condition'. In: *Journal of the Society of Naval Architects of Japan* 1990.168, pp. 141–148. DOI: 10.2534/jjasnaoe1968.1990.168_141.

Kolk, N. et al. (Jan. 2019). 'Case Study: Wind-Assisted Ship Propulsion Performance Prediction, Routing, and Economic Modeling'. In: *Power & Propulsion Alternatives for Ships 2019*. DOI: 10.3940/rina.ppa.2019.12.

Kramer, Jarle A. (2014). 'Hydrodynamic performance of sail-assisted merchant vessels'. In:

Lagemann, Benjamin (Apr. 2022). *Metocean download library*. URL: https://github.com/NTNU-IMT/Metocean.

Lindstad, Elizabeth et al. (2022). 'Reaching IMO 2050 GHG targets through Energy efficiency measures [unpublished article]'. In: *SNAME Maritime Convention 2022*.

Lloyd's Register Advisory Services BV (Jan. 2020). *Technology SkySails Propulsion*. URL: https://flettner.lr.org/ (visited on 19th Nov. 2021).

Lu, Ruihua and Jonas Ringsberg (Mar. 2020). 'Ship energy performance study of three wind-assisted ship propulsion technologies including a parametric study of the Flettner rotor technology'. In: *Ships and Offshore Structures* 15, pp. 249–258. DOI: 10.1080/17445302.2019.1612544.

Mackor, Rob and Tobias Pieffers (Jan. 2021). *Neptune Marine contracted to build futuristic Ariane rocket ship*. URL: https://www.projectcargojournal.com/shipping/2021/01/05/neptune-marine-contracted-to-build-futuristic-ariane-rocket-ship/ (visited on 30th May 2022).

Norsepower (Jan. 2021a). *RORO vessel*. URL: https://www.norsepower.com/roro/ (visited on 28th Sept. 2021).

— (2021b). *Technology*. URL: https://www.norsepower.com/technology/ (visited on 19th Oct. 2021).

Perez, Sergio, Changqian Guan and Alexander Mesaros (Aug. 2021). 'Economic viability of bulk cargo sailing ships'. In.

Prandtl, Ludwig and Albert Betz (1932). 'Ergebnisse der Aerodynamischen Versuchsanstalt zu Göttingen; IV. Lieferung'. In: *Kaiser Wilhelm Institute for Fluid Dynamics, Göttingen, DE*.

Da-Qing, L, Michael Leer-Andersen and Björn Allenström (2012). 'Performance and vortex formation of Flettner rotors at high Reynolds numbers'. In: *Proceedings of 29th Symposium on Naval Hydrodynamics*.

Reche-Vilanova, Martina, Heikki Hansen and Harry Bingham (June 2021). 'Performance Prediction Program for Wind-Assisted Cargo Ships'. In: *Journal of Sailing Technology* 6, pp. 91–117. DOI: 10.5957/jst/2021.6.1.91.

Sea-web (2022). *ship details IMO 9759252*. URL: https://maritime.ihs.com/Ships/Details/9759252 (visited on 26th Apr. 2022).

Seatrans (2021). *Rotorsail update*. URL: https://seatrans.no/news-2/ (visited on 1st June 2022).

Seddiek, Ibrahim S. and Nader R. Ammar (Feb. 2021). 'Harnessing wind energy on merchant ships: case study Flettner rotors onboard bulk carriers'. In: *Environmental Science and Pollution Research volume*, pp. 32695–32707. DOI: https://doi.org/10.1007/s11356-021-12791-3.

Selen, T. (2020). 'Simulating installation logistics for wind turbines using feeder vessels'. In: *NTNU*.

Ship and bunker (Apr. 2022). *Rotterdam Bunker Prices*. URL: https://shipandbunker.com/prices/emea/nwe/nl-rtm-rotterdam#MGO (visited on 23rd Apr. 2022).

SkySails (Sept. 2021). *Technology SkySails Propulsion*. URL: https://skysails-marine.com/technology.html (visited on 18th Nov. 2021).

Tillig, Fabian and Jonas W. Ringsberg (2020). 'Design, operation and analysis of wind-assisted cargo ships'. In: *Ocean Engineering* 211, p. 107603. ISSN: 0029-8018. DOI: https://doi.org/10.1016/j.oceaneng.2020.107603. URL: https://www.sciencedirect.com/science/article/pii/S0029801820306077.

Werner, Sofia, Da-Qing Li and Vendela Santén (2020). *A renaissance of wind-powered ships*. URL: https://www.sspa.se/renaissance-of-wind-powered-ships (visited on 22nd Mar. 2022).

Wikipedia (Aug. 2021a). *Ville De Bordeaux*. URL: https://en.wikipedia.org/wiki/Ville_de_Bordeaux (visited on 18th Nov. 2021).

— (2021b). *DynaRig*. Last checked on Des 9, 2021. URL: https://en.wikipedia.org/wiki/DynaRig (visited on 9th Dec. 2021).

Wind ship development corporation (1981). 'Wind propulsion for ships of the American merchant marine'. In: pp. 1–304.

Woodward, John et al. (1975). 'Feasibility of Sailing Ships for the American Merchant Marine'. In.

Appendix

A Retrieving weather data

```
from ReadDatabase import ReadDatabase
df = ReadDatabase('william_ais2.db')
df.reset_index(inplace=True, drop=True)

from MetoceanDownloader import MetoceanDownloader
downloader = MetoceanDownloader("", "")
import cftime
import pprint


# Writing to an excel sheet using Python
from xlwt import Workbook

# Workbook is created
wb = Workbook()

# add_sheet is used to create sheet.
sheet1 = wb.add_sheet('Sheet 1')

#defining labels to excel sheet
sheet1.write(0, 0, 'Time')
sheet1.write(0, 1, 'Latitude')
sheet1.write(0, 2, 'Longitude')
sheet1.write(0, 3, 'SOG')
sheet1.write(0, 4, 'Heading')
sheet1.write(0, 5, 'Mean wave direction')
sheet1.write(0, 6, 'Significant wave height')
sheet1.write(0, 7, 'Wave peak period')
sheet1.write(0, 8, 'Wind direction')
sheet1.write(0, 9, 'Wind speed')

for row in df.itertuples():
    latitude = row.lat
    longitude = row.lon
    time = row.dt
    year = time.year
    month = time.month
    day = time.day
    hour = time.hour
    minute = time.minute
    second = time.second
    time_input = cftime.datetime(year, month, day, hour, minute, \
```

```
    second)

    #Obtaining weather data
    requested_data = downloader.get_weather(time_input, latitude, \
    longitude)

    pp = pprint.PrettyPrinter(indent=4)
    pp.pprint(requested_data)

    ship_speed = row.sog
    ship_heading = row.heading
    wave_direction = int(requested_data['mean wave direction']['value'])
    wave_height = int(requested_data['significant wave height']['value'])
    wave_period = int(requested_data['wave peak period']['value'])
    wind_speed = int(requested_data['wind speed in 10m height']['value'])
    wind_direction = int(requested_data['wind direction in 10m height'] \
    ['value'])

    #writing to excel file
    sheet1.write(row.index + 1, 0, row.dt)
    sheet1.write(row.index + 1, 1, latitude)
    sheet1.write(row.index + 1, 2, longitude)
    sheet1.write(row.index + 1, 3, ship_speed)
    sheet1.write(row.index + 1, 4, ship_heading)
    sheet1.write(row.index + 1, 5, wave_direction)
    sheet1.write(row.index + 1, 6, wave_height)
    sheet1.write(row.index + 1, 7, wave_period)
    sheet1.write(row.index + 1, 8, wind_direction)
    sheet1.write(row.index + 1, 9, wind_speed)

wb.save('Test.xls')
```

B Combining weather data and effects from WASP

```
import pandas as pd
from xlwt import Workbook

#df = pd.read_csv('Results_operation.csv')
df = pd.read_csv('Resultater.csv')#importing csv file
df = df.dropna(subset = ['Time'], inplace=False)

#creating excel file
wb = Workbook()
# add_sheet is used to create sheet.
sheet1 = wb.add_sheet('Sheet 1')
#setting column headers
```

```
sheet1.write(0, 0, 'Time')
sheet1.write(0, 1, 'Latitude')
sheet1.write(0, 2, 'Longitude')
sheet1.write(0, 3, 'SOG')
sheet1.write(0, 4, 'Heading')
sheet1.write(0, 5, 'Wind_direction')
sheet1.write(0, 6, 'Wind_speed')
sheet1.write(0, 7, 'True_wind_angle')
sheet1.write(0, 8, 'Percent_saved')
sheet1.write(0, 9, 'Fuel_saved[kg/h]')
sheet1.write(0, 10, 'Effective_thrust[N]')
sheet1.write(0, 11, 'Required_power_ship[w]')
sheet1.write(0, 12, 'Saved_power_ship[W]')
sheet1.write(0, 13, 'Effective_rotor_power[W]')

data = pd.read_csv('All_cases7.csv') #importing csv file

#initial value
percent = 0
fuel = 0
n = 0

from Functions import WASP_Output

for row in df.itertuples():
    n = n + 1
    time = row.Time
    latitude = row.Latitude
    longitude = row.Longitude
    ship_speed = 14.4#row.SOG
    ship_heading = row.Heading
    wind_direction = row.Wind_direction
    wind_speed = row.Wind_speed
    true_wind_angle = row.True_wind_angle
    saved_power_ship, effective_rotor_power, required_power_ship, \
    effective_thrust, saved_percent, saved_fuel = \
    WASP_Output(data, true_wind_angle, ship_heading, ship_speed, \
    wind_speed)

    #writing to excel sheet
    sheet1.write(row.Index + 1, 0, time)
    sheet1.write(row.Index + 1, 1, latitude)
    sheet1.write(row.Index + 1, 2, longitude)
    sheet1.write(row.Index + 1, 3, ship_speed)
    sheet1.write(row.Index + 1, 4, ship_heading)
    sheet1.write(row.Index + 1, 5, wind_direction)
    sheet1.write(row.Index + 1, 6, wind_speed)
    sheet1.write(row.Index + 1, 7, true_wind_angle)
```

```
    sheet1.write(row.Index + 1, 8, saved_percent)
    sheet1.write(row.Index + 1, 9, saved_fuel)
    sheet1.write(row.Index + 1, 10, effective_thrust)
    sheet1.write(row.Index + 1, 11, required_power_ship)
    sheet1.write(row.Index + 1, 12, saved_power_ship)
    sheet1.write(row.Index + 1, 13, effective_rotor_power)
    percent = percent + saved_percent
    fuel = fuel + saved_fuel
    wb.save('Results_all.xls')

#converting excel file to csv
read_file = pd.read_excel(r'Results_all.xls')
read_file.to_csv(r'Results_all.csv', index=True, header=True)

Average_percent = percent/n #average fuel savings in percent
Average_fuel_savings = fuel/n #average fuel savings in kg/h
print(Average_percent)
print(Average_fuel_savings)
```

C Operational modes

```
import pandas as pd
from Functions import WASP_Output_Operation
from Functions import Distance
from xlwt import Workbook

df = pd.read_csv('Resultater.csv')
data = pd.read_csv('All_cases11.csv')

#creating excel file
wb = Workbook()
# add_sheet is used to create sheet.
sheet1 = wb.add_sheet('Sheet 1', cell_overwrite_ok=True)
#setting column headers
sheet1.write(0, 0, 'Time')
sheet1.write(0, 1, 'Latitude')
sheet1.write(0, 2, 'Longitude')
sheet1.write(0, 3, 'SOG')
sheet1.write(0, 4, 'Heading')
sheet1.write(0, 5, 'Wind_direction')
sheet1.write(0, 6, 'Wind_speed')
sheet1.write(0, 7, 'True_wind_angle')
sheet1.write(0, 8, 'Percent_saved')
sheet1.write(0, 9, 'Fuel_saved[kg/h]')
sheet1.write(0, 10, 'Time difference [h]')
sheet1.write(0, 11, 'Required_power_ship[w]')
```

```
sheet1.write(0, 12, 'Saved_power_ship[W]')
sheet1.write(0, 13, 'Fuel_consumption_[kg/h]')


def main(difference, Fuel_consumption):
    time = 0
    group_i = group.get_group(i)
    count = 0
    for row in group_i[:-1].itertuples():
        latitude = row.Latitude
        longitude = row.Longitude
        latitude_2 = group_i.loc[row.Index + 1, 'Latitude']
        longitude_2 = group_i.loc[row.Index + 1, 'Longitude']
        ship_heading = row.Heading
        wind_direction = row.Wind_direction
        wind_speed = row.Wind_speed
        true_wind_angle = row.True_wind_angle
        ship_speed, fuel_consumption, saved_power_ship, \
        effective_rotor_power, required_power_ship, effective_thrust,\
        saved_percent, saved_fuel = \
            WASP_Output_Operation(data, true_wind_angle, ship_heading, \
            wind_speed, difference)

        distance = Distance(latitude, longitude, latitude_2, longitude_2)
        time = time + (distance / ship_speed) / 24  # datetime at location
        time_old = row.Time #datetime at location without WASP
        Fuel_consumption = Fuel_consumption + fuel_consumption

        sheet1.write(row.Index + 1, 0, time_old)
        sheet1.write(row.Index + 1, 1, latitude)
        sheet1.write(row.Index + 1, 2, longitude)
        sheet1.write(row.Index + 1, 3, ship_speed)
        sheet1.write(row.Index + 1, 4, ship_heading)
        sheet1.write(row.Index + 1, 5, wind_direction)
        sheet1.write(row.Index + 1, 6, wind_speed)
        sheet1.write(row.Index + 1, 7, true_wind_angle)
        sheet1.write(row.Index + 1, 8, saved_percent)
        sheet1.write(row.Index + 1, 9, saved_fuel)
        #sheet1.write(row.Index + 1, 10, time_new_delta)
        sheet1.write(row.Index + 1, 11, required_power_ship)
        sheet1.write(row.Index + 1, 12, saved_power_ship)
        sheet1.write(row.Index + 1, 13, fuel_consumption)
        time_last = group_i.loc[row.Index + 1, 'Time']
        time_first = group_i['Time'].values[0]
        index = row.Index

    #Calculating the time difference
    time_delta = time_last - time_first - time
```

```
    print(time_delta)
    #if the time used for the voyage was within acceptable limit
    if (time_delta <= slack) & (time_delta >= -slack):
        print(index)
        wb.save('Results_operation.xls')
        return
    #reduce speed if the vessel sailed too fast
    if time_delta > slack:
        difference = difference - 0.25
        main(difference, fuel_consumption)
    #increase speed if vessel sailed to slow
    if time_delta < -slack:
        difference = difference + 0.25
        main(difference, fuel_consumption)
    return

slack = 0.25 #6 hour slack so the code can find a solution
time_count = 0 #initial value
Fuel_consumption = 0 #initial value
#dividing the voyages into bin based on datetime:
df['bin'] = pd.cut(x=df['Time'],
                   bins=[43839, 43855, 43891, 43913, 43949, 43980, \
                   44004, 44034, 44059, 44080, 44096, 44106, 44115, \
                   44131, 44159, 44178, 44193],
                   include_lowest=True)
group = df.groupby('bin')
#calling on main function for every voyage
for i in group.groups:
    difference = 0
    n = main(difference, Fuel_consumption)

#saving results
read_file = pd.read_excel(r'Results_operation.xls')
read_file.to_csv(r'Results_operation.csv', index=True, header=True)
```

D Functions

```
#Function that calculates WASP performance based on inputs
def WASP_Output(dataframe, wind_direction, ship_heading, ship_speed, \
    wind_speed):
    true_wind_angle = wind_direction - ship_heading
    if true_wind_angle < 0:
        true_wind_angle = true_wind_angle + 360
    if true_wind_angle > 180:
        true_wind_angle = 360 - true_wind_angle
```

```
    # rounding of to nearest column value
    #nearest 0.25 and converting to m/s
    ship_speed_rounded = round(ship_speed * 4) / 4
    #nearest integer
    wind_speed_rounded = round(wind_speed)
    #nearest even number
    true_wind_angle_rounded = round(true_wind_angle / 2) * 2

    # Finding the row corresponding to the given conditions
    corresponding_row = dataframe.loc[
        (dataframe['Ship speed [kn]'] == ship_speed_rounded) & \
        (dataframe['True wind speed [m/s]'] == wind_speed_rounded) & \
        (dataframe['True wind angle [deg]'] == true_wind_angle_rounded)]
    #extracting values from the row
    saved_power_ship = corresponding_row['Saved power ship[W]'].values[0]
    effective_rotor_power = \
    corresponding_row['Effective rotor power [W]'].values[0]
    required_power_ship = \
    corresponding_row['Effective rotor power [W]'].values[0]
    effective_thrust = corresponding_row['Effective thrust [N]'].values[0]
    saved_percent = corresponding_row['Percental savings'].values[0]
    saved_fuel = \
    corresponding_row['Fuel saved [kg/h]'].values[0]/1000 #converting to kg

    return saved_power_ship, effective_rotor_power, required_power_ship, \
    effective_thrust, saved_percent, saved_fuel

#function that calculates distance between two coordinates
#could also use geopy.distance.geodesic, but running time is doubled
def Distance(lat1, lon1, lat2, lon2):
    import numpy as np
    R = 6371 * 0.539956803 # Earth radius in nautical miles
    theta1 = lat1 * np.pi/180 # theta, lambda in radians
    theta2 = lat2 * np.pi/180
    deltatheta = (lat2-lat1) * np.pi/180
    deltalambda = (lon2-lon1) * np.pi/180
    a = np.sin(deltatheta/2) * np.sin(deltatheta/2) + np.cos(theta1)  \
    * np.cos(theta2) * np.sin(deltalambda/2) * np.sin(deltalambda/2)
    c = 2 * np.arctan2(np.sqrt(a), np.sqrt(1-a))
    distance = c * R
    return distance

# Function that create a list of colors to use for plotting.
def linePlottingColorsPercent(percental_saving):
    speed = percental_saving
    a = 25
    b = 10
    if speed > a:
```

```
        color = "#0000FF"  # blue
    elif speed <= a and speed > b: # <14, 16]
        color = "#00b500"  # green
    elif speed <= b and speed > 0: # [0, 10]
        color = "#FFFF00" # yellow
    else:
        color = "#FF0000" # red
    return color

#Function that calculates WASP performance based on inputs
def WASP_Output_Operation(dataframe, wind_direction, ship_heading,\
wind_speed, difference):
    true_wind_angle = wind_direction - ship_heading
    if true_wind_angle < 0:
        true_wind_angle = true_wind_angle + 360
    if true_wind_angle > 180:
        true_wind_angle = 360 - true_wind_angle

    # rounding of to nearest column value
    # nearest integer
    wind_speed_rounded = round(wind_speed)
    # nearest even number
    true_wind_angle_rounded = round(true_wind_angle / 2) * 2

    #Finding the row corresponding to the given conditions
    corresponding_row = dataframe.loc[(dataframe['Ship speed [kn]'] == 16)
         & (dataframe['True wind speed [m/s]'] == wind_speed_rounded) \
         & (dataframe['True wind angle [deg]'] == true_wind_angle_rounded)]
    #corresponding_rows.sort_values(by='Ship speed [kn]', axis=0, \
    ascending=False, inplace=True)

    saved_percent = corresponding_row['Percental savings'].values[0]
    #Increasing ship speed when wind conditions are benificial
    ship_speed = 10 + saved_percent*0.3 + difference
    #nearest 0.25 and converting to m/s
    ship_speed_rounded = round(ship_speed * 4) / 4

    corresponding_row = dataframe.loc[\
    (dataframe['Ship speed [kn]'] == ship_speed_rounded) \
    & (dataframe['True wind speed [m/s]'] == wind_speed_rounded) \
    & (dataframe['True wind angle [deg]'] == true_wind_angle_rounded)]

    saved_power_ship = corresponding_row['Saved power ship[W]'].values[0]
    effective_rotor_power = \
    corresponding_row['Effective rotor power [W]'].values[0]
    required_power_ship = \
    corresponding_row['Effective rotor power [W]'].values[0]
    effective_thrust = \
```

```
    corresponding_row['Effective thrust [N]'].values[0]
    saved_percent = corresponding_row['Percental savings'].values[0]
    saved_fuel = \
    corresponding_row['Fuel saved [kg/h]'].values[0]/1000
    fuel_consumption = \
    corresponding_row['Fuel consumption [kg/h]'].values[0]

    return ship_speed_rounded, fuel_consumption, saved_power_ship, \
    effective_rotor_power, required_power_ship, effective_thrust, \
    saved_percent, saved_fuel

#Author: Andreas Isaksen, andrisa@stud.ntnu.no
# Function that create a list of colors to use for plotting.
def linePlottingColorsSpeed(speed):
    a = 18
    b = 16
    c = 14
    d = 10
    if speed > a:
        color = "#0000FF" #blue
    elif speed <= a and speed > b: # <18, 16]
        color = "#00b500"  # green
    elif speed <= b and speed > c: # <14, 16]
        color = "#FFFF00" # yellow
    elif speed <= c and speed > d: # <10, 14]
        color = "#FF0000" # red
    elif speed <= d and speed >= 0: # [0, 10]
        color = "#FF00ae"  # pink
    else:
        color = "#000000" #black
    return color
```

E Fuel savings in percent

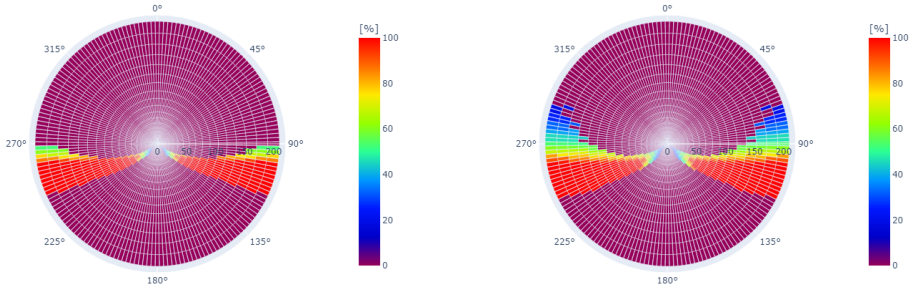

(a) 8 knots

(b) 10 knots

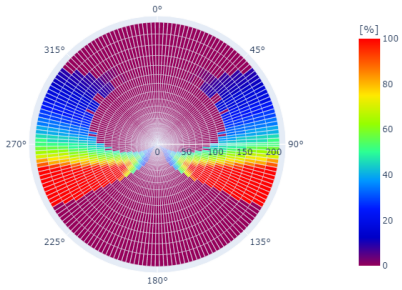

(c) 12 knots

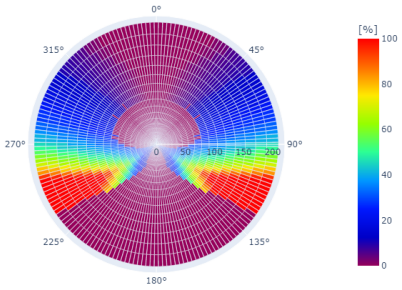

(d) 14 knots

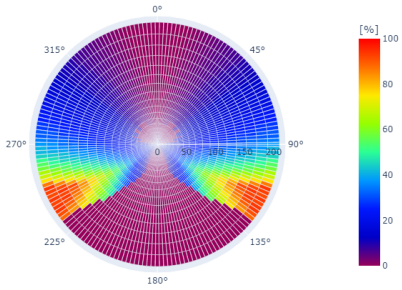

(e) 16 knots

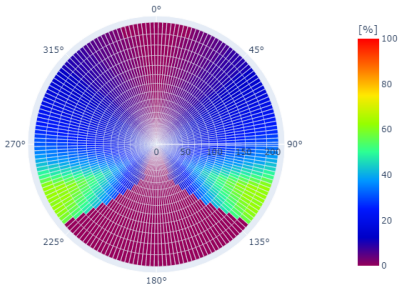

(f) 18 knots

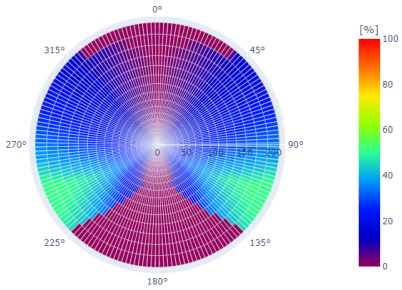

(g) 20 knots

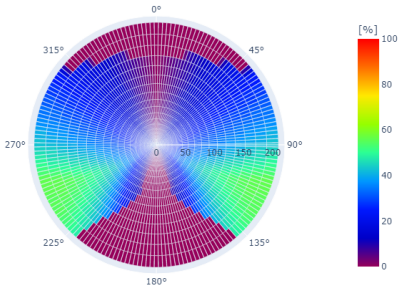

(h) 22 knots

Figure 1: Polar plots of fuel savings in percent

F Effective thrust

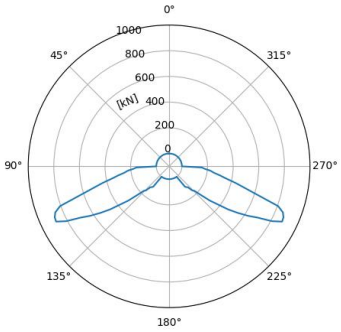

(a) 8 knots

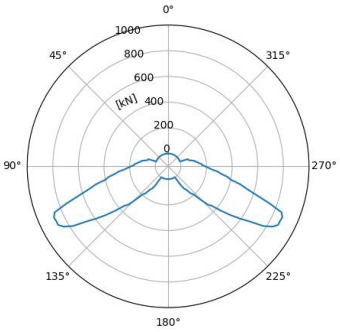

(b) 10 knots

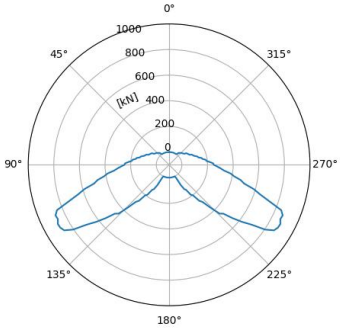

(c) 12 knots

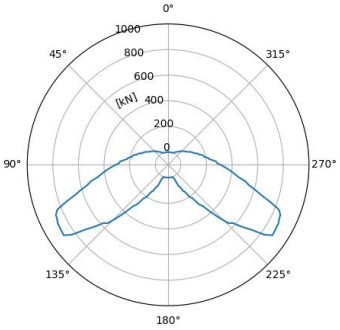

(d) 14 knots

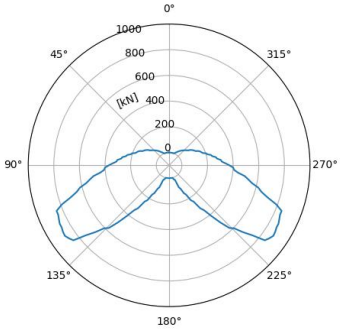

(e) 16 knots

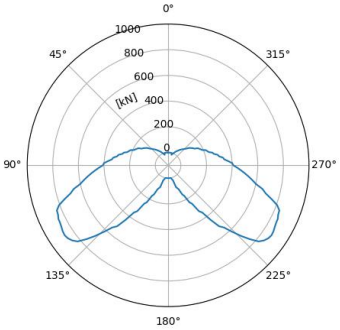

(f) 18 knots

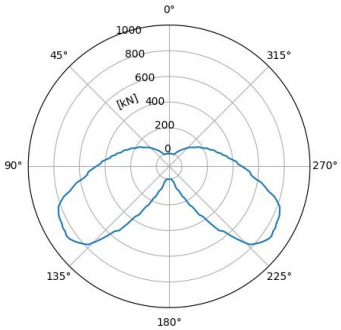

(g) 20 knots

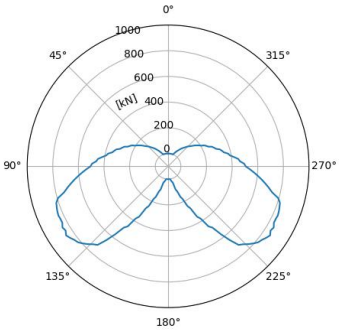

(h) 22 knots

Figure 2: Effective thrust

G Effective power

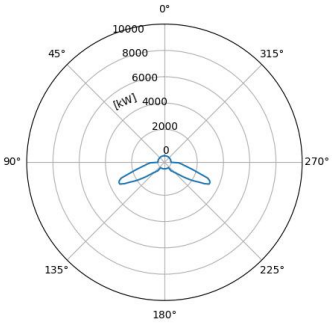

(a) 8 knots

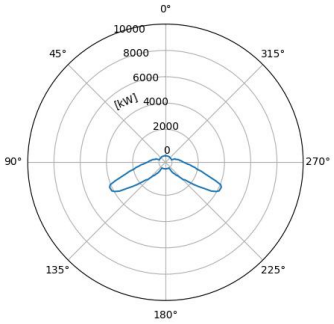

(b) 10 knots

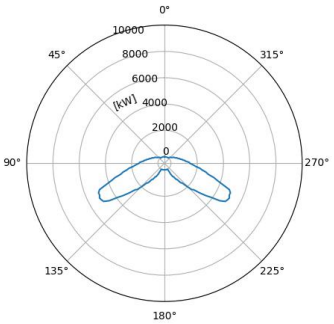

(c) 12 knots

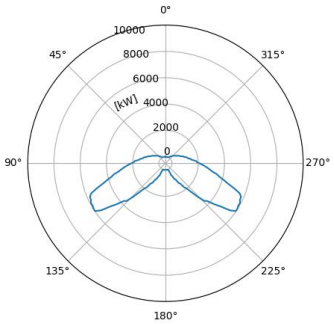

(d) 14 knots

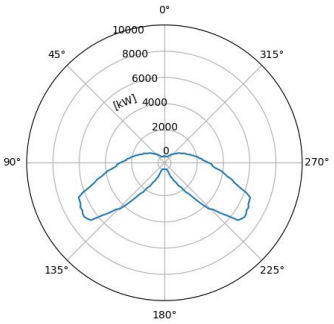

(e) 16 knots

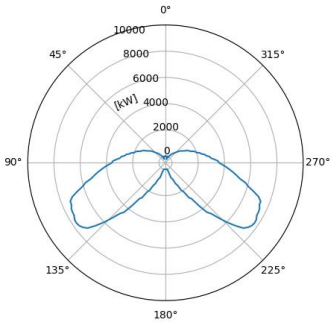

(f) 18 knots

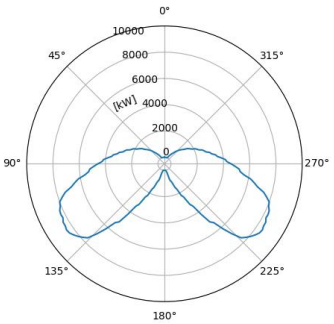

(g) 20 knots

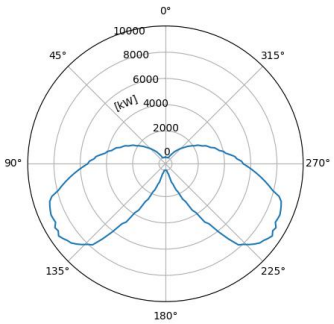

(h) 22 knots

Figure 3: Effective power

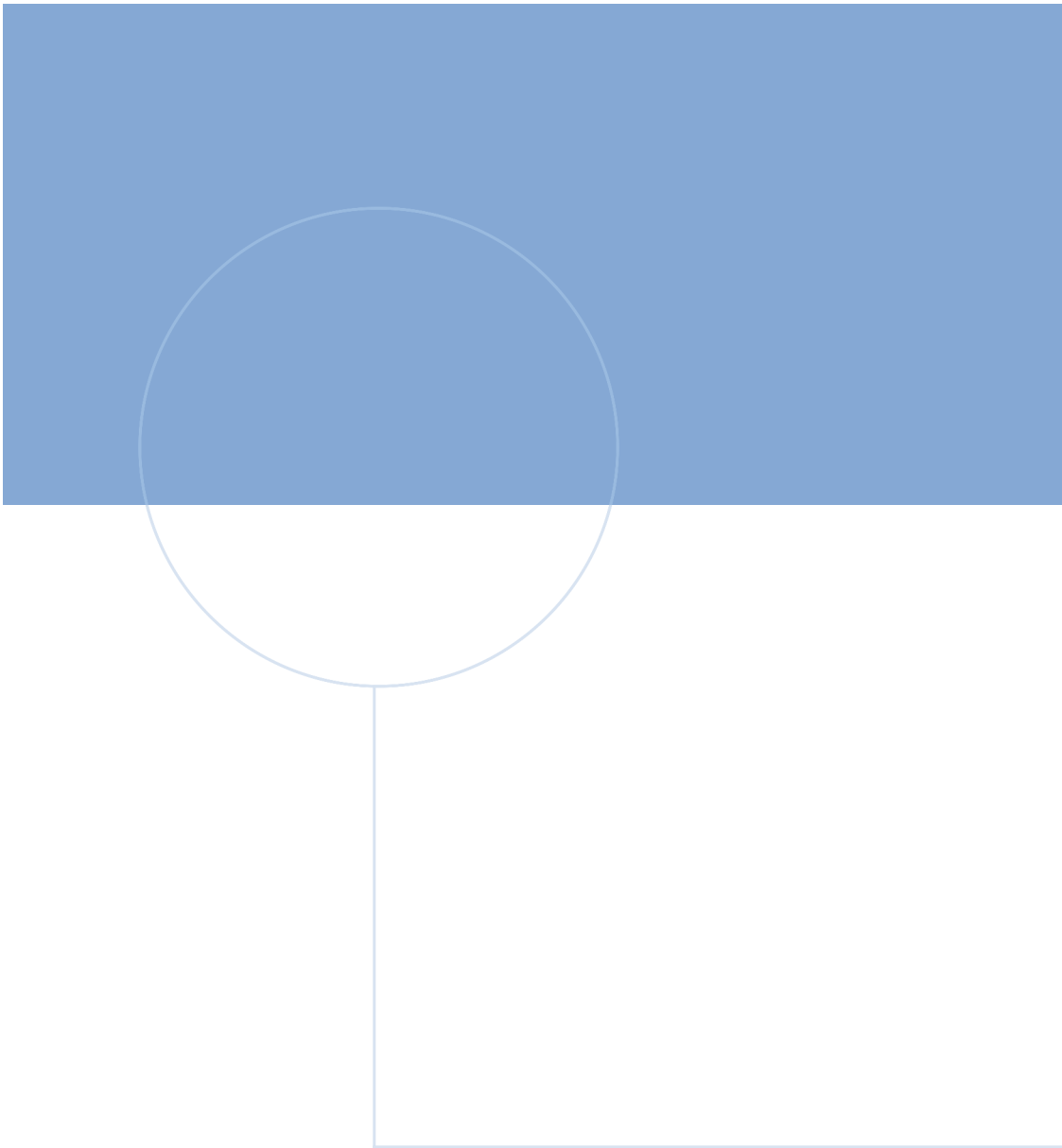

NTNU

Norwegian University of
Science and Technology